sp2 Carbon-Conjugated Covalent Organic Frameworks: Synthesis, Properties, and Applications

Journal:	*Materials Chemistry Frontiers*
Manuscript ID	QM-REV-01-2021-000015.R1
Article Type:	Review Article
Date Submitted by the Author:	27-Jan-2021
Complete List of Authors:	Li, Xinle; Clark Atlanta University

SCHOLARONE™
Manuscripts

ARTICLE

sp^2 Carbon-Conjugated Covalent Organic Frameworks: Synthesis, Properties, and Applications

Received 00th January 20xx,
Accepted 00th January 20xx

DOI: 10.1039/x0xx00000x

Xinle Li*[a]

Covalent organic frameworks (COFs) represent an emerging class of well-ordered porous materials that precisely reticulate organic units into extended networks and have been at the forefront of porous materials research over the past decade. In the quest to expand the reticular chemistry and develop next-generation COFs with peculiar materials properties, sp^2 carbon-conjugated COFs (sp^2c-COFs) have garnered a surge of interest since their inception in 2016 due to the unparalleled features of continuous π-conjugation, high crystallinity, permanent porosity, unique optoelectronic properties, and extraordinary chemical stability. A rapidly growing number of 2D sp^2c-COFs (more than 40 in total within just 4 years) have been hitherto constructed and broadly exploited in various areas. In this review, we scrutinize the design principles, synthetic routes, key features, and mechanistic investigations of sp^2c-COFs. We survey the advances in their broad applications spanning heterogeneous catalysis, radionuclides sequestration, lithium-ion batteries, supercapacitors, and optical applications, as well as rationalize their superior performance against structurally analogous imine-linked COFs. We further discuss the unsettled scientific challenges and provide future perspectives of sp^2c-COFs.

Introduction

The clear-cut assembly of molecular subunits into periodically ordered architectures has been long sought in materials chemistry since it enables the predictive synthesis and rational improvement of new materials as well as furnishes unprecedented properties and functions.[1] Despite enormous strides in organic polymer chemistry over the past century, it has remained a formidable synthetic challenge to construct well-defined high-order organic polymers. This long-standing challenge was tackled with the advent of covalent organic frameworks (COFs) in 2005.[2] COFs are an emerging class of two- or three-dimensional (2D or 3D) porous crystalline solids formed by covalently stitching organic building blocks into extended networks.[3] The inherent high crystallinity, large surface areas, ultralow density, and predesignable architectures,[4] render COFs as a compelling molecular platform in a plethora of applications ranging from gas separation, catalysis, sensing, water remediation, biomedicine, supercapacitors, and optoelectronics.[5-8]

The construction of COFs typically hinges on error-correction and self-healing processes to achieve the most thermodynamically stable crystalline products,[9] with a few exceptions that 2D COFs can be obtained by irreversible reactions either on confined interfaces,[10-12] or using rigid directional monomers.[13] The common reliance upon reversible reactions intrinsically limits the chemical stability and structural complexity of COFs, which are considerable roadblocks that hamper the full implementation of these intriguing materials.[14] To alleviate these shortcomings, tremendous efforts have been invested in new linkage chemistries that primarily govern the properties of COFs.[15] Consequently, the past decade has witnessed a rapid expansion of COF linkages from boronate ester, triazine, imine, imide, olefin, aryl ether to ester, benzofuran, and pyrimidazole. A handful of new and robust linkages have been incorporated into COFs by (1) single-step reactions;[16-20] (2) cascade reversible-irreversible transformations;[21-24] (3) postsynthetic linkage conversion to transform labile linkages into irreversible units.[25-28] The booming development of novel linkages has flourished unparalleled properties and functions of COFs as well as greatly expanded the scope of reticular chemistry.

Amongst the COFs with emerging linkages, sp^2 carbon-conjugated COFs (aka olefin- or vinylene-linked COFs[29]) are of substantial interest since the innate sp^2 C=C linkages simultaneously enhance both chemical stability and in-plane π-electron delocalization of COFs, which are downsides of the current COF systems. Further, the straightforward *de novo* synthesis along with broad monomer scope and high reaction efficiency adds great zeal to this novel class of COFs. The first sp^2 carbon-conjugated COF (termed sp^2c-COF) was developed in 2016 by using a base-catalyzed Knoevenagel condensation.[30] Later in 2017, an unprecedented ferromagnetic phase transition and a drastic conductivity enhancement upon iodine doping was uncovered in a sp^2c-COF otherwise not observed in its amorphous counterpart and imine-linked COF analog.[31-33] Since these landmark reports, sp^2c-COFs have undergone striking development evident by the rapidly increasing number of publications each year (Scheme 1), and over 40 sp^2c-COFs with varying pore metrics have been reported within just 4 years, rendering them among the most emerging next-generation COFs with highly sought-after material properties. A timeline showing some representative breakthroughs in the exploration of sp^2c-COFs is illustrated in Scheme 1. Despite numerous recent COF reviews that span the design,[34-36] synthesis,[37] and applications,[38-41] a comprehensive review that delineates the latest advances in sp^2c-COFs remains an uncharted territory and is urgently demanded.

[a] Department of Chemistry, Clark Atlanta University, Atlanta, GA 30314, United States

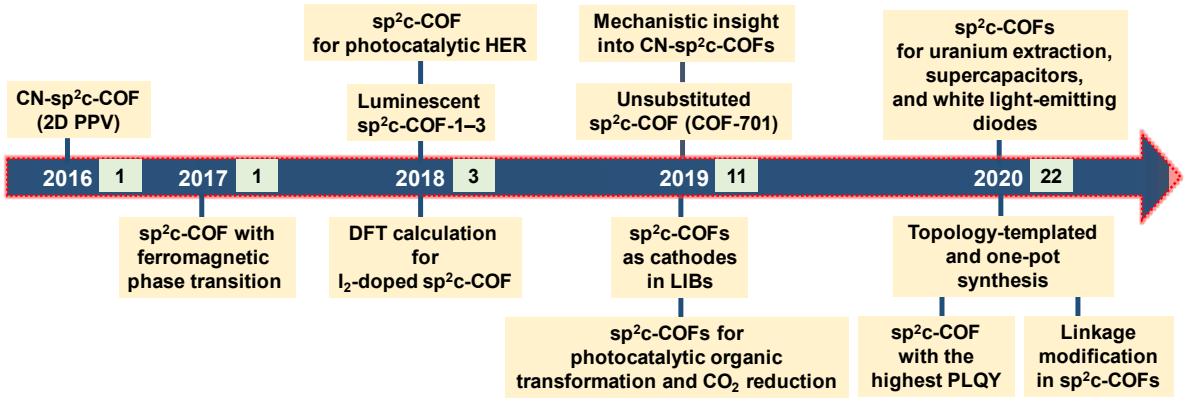

Scheme 1. Timeline of significant advances in the development of sp^2 carbon-conjugated COFs with an increasing number of yearly publications highlighted in olive green.

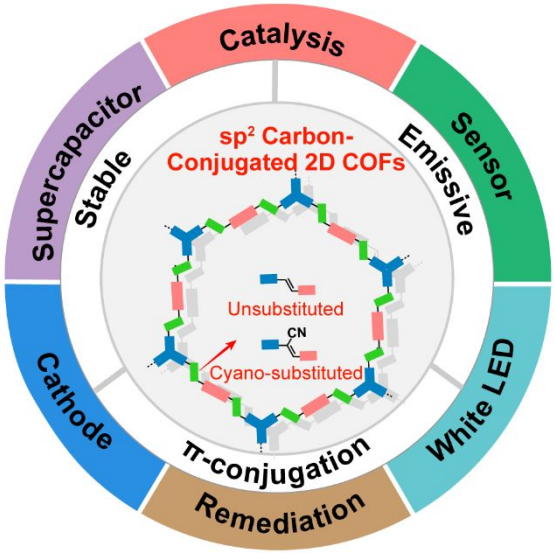

Scheme 2. The category, key structural merits, and widespread applications of sp^2 carbon-conjugated 2D COFs.

Herein we present the first systematic overview of the research advances in sp^{2}c-COFs since their dawn in 2016 (Scheme 2). We disclose the design principles and synthetic routes toward sp^{2}c-COFs through Knoevenagel condensation, Aldol condensation, and Horner-Wadsworth-Emmons reaction. A comprehensive summary of reported sp^{2}c-COFs is listed in Table 1 in chronological order. We highlight the advantages of sp^{2}c-COFs over other prototypical COFs concerning chemical stability, crystallinity, structural complexity, π-conjugation, and photoluminescence; deliberate the latest progress of mechanistic studies; scrutinize the applications of sp^{2}c-COFs in various domains spanning heterogeneous catalysis, uranium capture, energy storage, and optical applications; underscore their superior performance over imine-linked COF analogs; discuss the remaining challenging issues, and provide outlooks for sp^{2}c-COFs in cutting-edge research directions.

2. Structural design, synthesis, advantage, and mechanistic study of sp^{2}c-COFs

2.1 Structural design

The lattice symmetry, functionality, and pore size of sp^{2}c-COFs can be well predesigned following the principle of the topology diagram, which directs the orientation of covalent linkages and secures the polymer growth. The reactive sites of rigid monomers are oriented in a specific geometry and regulate the spatial orientation and position of the next reactive groups, leading to the formation of distinct polygon skeletons.[42] As shown in Fig. 1A, the combination of [C_2 + C_3] or [C_3 + C_3] monomers produces hexagonal 2D COFs; Tetragonal COFs are generated by a combination of [C_4 + C_2] monomers while triangular COFs with micropores are formed from the [C_6 + C_2] diagram. A [C_2 + C_2] combination is of particular interest since it can produce single-pore rhombic COFs and kagome-type COFs with dual-pore structures.

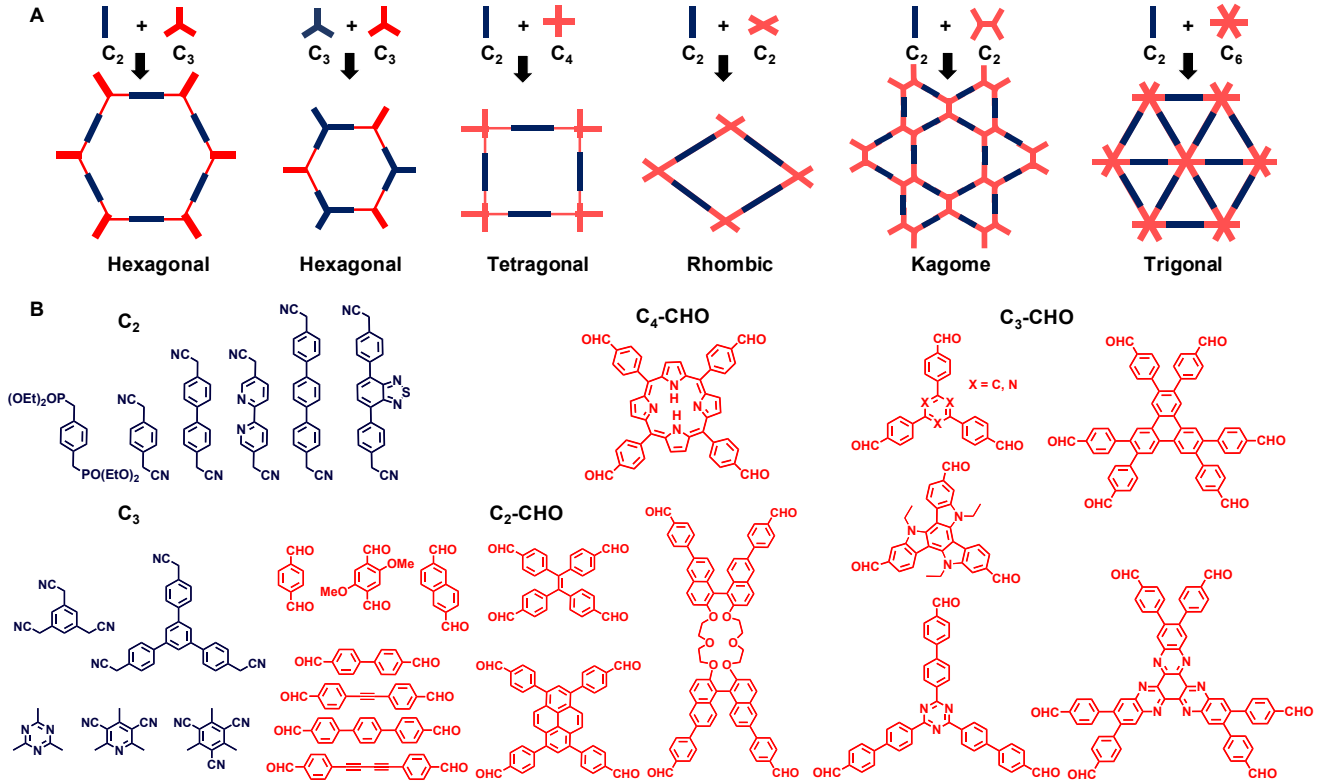

Fig. 1. A. Typical topology diagram for the design of 2D sp^{2}c-COFs; B. Reported building blocks with different reactive sites for the synthesis of sp^{2}c-COFs to date.

2.2 Synthetic route to sp^{2}c-COFs

sp^{2}c-COFs are mainly prepared by the Knoevenagel condensation and very few are obtained via Aldol condensation and Horner-Wadsworth-Emmons reaction. Knoevenagel condensation, which is a cascade nucleophilic addition-dehydration reaction between an activated methylene and an aldehyde or ketone, represents a proven strategy to yield C=C bonds and has been broadly exploited in the synthesis of vinyl-based porous polymers.[43-46] Fig. 1B illustrates the reported monomers with different reactive sites and functionalities for the synthesis of sp^{2}c-COFs. Based on the substitution of sp^2 C=C linkages, sp^{2}c-COFs can be categorized into two subclasses: cyano-substituted and unsubstituted sp^{2}c-COFs. Cyano-substituted sp^{2}c-COFs are obtained by the topology-directed polymerization between benzylnitriles and aryl aldehydes monomers. However, the strong electron-withdrawing cyano groups appended to C=C bonds induce structural twisting arising from the steric hindrance as well as make the linkage reversible and compromise their stability. To this end, unsubstituted sp^{2}c-COFs emerged later (2019) by reticulating aryl aldehydes with electron-deficient mesitylene monomers or phosphonates.

sp^{2}c-COF synthesis is exclusively performed via the conventional solvothermal approach, in which monomers are mixed in a sealed vessel under vacuum or an inert atmosphere for predesignated reaction times (3-5 days) at elevated temperature (80-180 ^{o}C) with the aid of catalysts. The formation of crystalline sp^{2}c-COFs highly depends on modulating the thermodynamic equilibrium of covalent reactions by varying the synthetic parameters systematically. The appropriate selection of catalysts is paramount for the synthesis of COFs. Bases are the most common catalysts in the synthesis of sp^{2}c-COFs via Knoevenagel condensation and Horner-Wadsworth-Emmons reaction whereas very limited sp^{2}c-COFs used Brønsted acid (i.e., trifluoroacetic acid) as a catalyst through Aldol condensation.[47-48] Among the base catalysts, anhydrous or aqueous alkaline bases (e.g., Cs_2CO_3, NaOH, 4M KOH) and organic bases (e.g., DBU, TBAH, piperidine) have been widely utilized. Besides, solvent combinations and ratios are crucial to obtain high-quality sp^{2}c-COFs. In addition to the direct solvothermal synthesis, a topology-templated polymerization strategy opens up new avenues to divergent sp^{2}c-COFs by using imine-linked 2D COFs as seed and template.[49] Moreover, the high cost of 2,4,6-trimethyl-1,3,5-triazine monomer motivated researchers to alternatively synthesize unsubstituted sp^{2}c-COFs through a one-pot cascade reaction that combines cyclotrimerization of inexpensive acetonitrile and subsequent Aldol condensation with aldehydes, which is appealing from the viewpoint of cost, energy, and time.[50] By virtue of the reticular chemistry principle and evolving synthetic strategies, the topology-directed polymerizations of monomers with C_2, C_3, and C_4 geometries gave rise to more than 40 sp^{2}c-COFs adopting various lattices (i.e.,

trigonal, tetragonal, hexagonal, rhombic, and kagome), micro-to-meso pores and diverse functionalities (Table 1).

Table 1. The summary of the reported sp^{2}c-COFs up to date.[a]

sp^{2}c-COFs	Combination	Solvent	Catalyst	Temperature /Time	BET surface area	Year	Ref.
Cyano-substituted sp^2-carbon Conjugated COFs							
2DPPV	$C_3 + C_2$	o-DCB	Cs_2CO_3 (s)	150 °C/3 d	472 m^2 g^{-1}	2016	30
sp^{2}c-COF	$C_2 + C_2$	Mesitylene/dioxane (1/5)	4M NaOH	90 °C /3 d	692 m^2 g^{-1}	2017	31
sp^{2}c-COF sp^{2}c-COF-2 sp^{2}c-COF-3	$C_2 + C_2$	Dioxane Dioxane o-DCB	4M KOH 4M KOH 1M TBAH	90 °C /3 d 110 °C /3 d 120 °C /3 d	322 m^2 g^{-1} 613 m^2 g^{-1} 737 m^2 g^{-1}	2018	63
2D-CN-PPV-1 2D-CN-PPV-2	$C_3 + C_3$ $C_3 + C_2$	o-DCB	Cs_2CO_3 (s)	120 °C/3 d	301 m^2 g^{-1} 638 m^2 g^{-1}	2019	71
Bpy-sp^{2}c-COF	$C_2 + C_2$	o-DCB/*n*-BuOH (1/1)	4M NaOH	120 °C /3 d	432 m^2 g^{-1}	2019	93
Por-sp^{2}c-COF	$C_4 + C_2$	o-DCB	5M DBU	80 °C /3 d	689 m^2 g^{-1}	2019	96
TP-COF	$C_3 + C_2$	Dioxane	Cs_2CO_3 (s)	120 °C/3 d	232 m^2 g^{-1}	2019	99
CCP-HATN	$C_3 + C_2$	DMAc/o-DCB (1/1)	Cs_2CO_3 (s)	120 °C/3 d	317 m^2 g^{-1}	2019	119
sp^{2}c-COF-4 sp^{2}c-COF-5	$C_3 + C_2$ $C_2 + C_2$	o-DCB/EtOH (1/1) with COF templates	4M KOH	120 °C /3 d	369 m^2 g^{-1} 348 m^2 g^{-1}	2020	49[b]
2D CCP-1 2D CCP-2	$C_3 + C_2$	DMAc/o-DCB (1/1)	0.1M Cs_2CO_3	120 °C /3 d	336 m^2 g^{-1} 102 m^2 g^{-1}	2020	64
2D CCP-Th 2D CCP-BD	$C_3 + C_2$	DMAc/o-DCB (3/7) DMAc/o-DCB (1/1)	0.1M NEt_4OH 0.1 M Cs_2CO_3	150 °C /3 d 120 °C /3 d	290 m^2 g^{-1} 441 m^2 g^{-1}	2020	90
sp^{2}c-COF$_{dpy}$ (Bpy-sp^{2}c-COF)	$C_2 + C_2$	Dioxane	4M KOH	110 °C /3 d	572 m^2 g^{-1}	2020	94
Py-BSZ-COF	$C_2 + C_2$	o-DCB	1M TBAH	120 °C /3 d	600 m^2 g^{-1}	2020	98
TFPT-BTAN	$C_3 + C_3$	o-DCB	4M DBU	90 °C /5 d	1062 m^2 g^{-1}	2020	108
NDA-TN BDA-TN	$C_3 + C_2$	o-DCB/*n*-BuOH (9/1)	5M NaOH	120 °C /3 d	1124 m^2 g^{-1} 1070 m^2 g^{-1}	2020	113
ED-TN BD-TN	$C_3 + C_2$	o-DCB/*n*-BuOH (3/7)	KOH (s)	120 °C /4 d	836 m^2 g^{-1} 940 m^2 g^{-1}	2020	115

This journal is © The Royal Society of Chemistry 20xx

Please do not adjust margins

cyano-sp^{2}c-COF (2DPPV)	$C_3 + C_2$	o-DCB/*n*-BuOH (1/4)	Cs_2CO_3 (s)	120 °C/3 d	327 $m^2 g^{-1}$	2020	127
CCOF 17 CCOF 18	$C_2 + C_2$	MeOH/dioxane (1/1)	4M KOH	120 °C/4 d	/	2020	129
Unsubstituted sp^2-carbon Conjugated COFs							
COF-701	$C_3 + C_2$	Mesitylene/dioxane /CH_3CN (1/1/0.1)	TFA	150 °C /3 d	1366 $m^2 g^{-1}$	2019	47[c]
V-COF-1 (g-$C_{18}N_3$-COF) V-COF-2 (g-$C_{33}N_3$-COF)	$C_3 + C_2$	MeOH/mesitylene (7/1 or 1/1)	NaOH (s)	180 °C /4 d	1341 $m^2 g^{-1}$ 627 $m^2 g^{-1}$	2019	29
COF-1 (g-$C_{18}N_3$-COF) COF-2 COF-3	$C_3 + C_2$	Dioxane/EtOH	1M NaOH	100 °C /3 d	880 $m^2 g^{-1}$	2019	62
g-$C_{40}N_3$-COF g-$C_{31}N_3$-COF g-$C_{37}N_3$-COF	$C_3 + C_2$ $C_3 + C_3$	DMF	Piperidine	150 °C /3 d	1235 $m^2 g^{-1}$ 864 $m^2 g^{-1}$ 1012 $m^2 g^{-1}$	2019	85
g-$C_{18}N_3$-COF g-$C_{33}N_3$-COF	$C_3 + C_2$ $C_3 + C_3$	o-DCB/*n*-BuOH (3/7)	KOH (s) NaOEt (s)	120 °C /3 d	1170 $m^2 g^{-1}$ 752 $m^2 g^{-1}$	2019	88
g-$C_{34}N_6$-COF	$C_3 + C_3$	DMF	Piperidine	180 °C /3 d	1003 $m^2 g^{-1}$	2019	125
TTO-COF (TM-TPT)	$C_3 + C_3$	Mesitylene/dioxane /CH_3CN (1/1/0.1)	TFA	150 °C /3 d	390 $m^2 g^{-1}$	2020	48[c]
COF-701 g-$C_{18}N_3$-COF	$C_3 + C_2$ $C_3 + C_3$	MeOH/CH_3CN (1/1)	TFA	120 °C /3 d	736 $m^2 g^{-1}$ 790 $m^2 g^{-1}$	2020	50[d]
2D-PPQV1 2D-PPQV2	$C_3 + C_2$	DMAc/mesitylene (1/1)	Cs_2CO_3 (s)	120 °C /3 d	440 $m^2 g^{-1}$ 100 $m^2 g^{-1}$	2020	72[e]
g-$C_{54}N_6$-COF g-$C_{52}N_6$-COF	$C_3 + C_3$	DMF	Piperidine	180 °C /3 d	855 $m^2 g^{-1}$ 1000 $m^2 g^{-1}$	2020	89
COF-p-3Ph COF-p-2Ph COF-m-3Ph	$C_3 + C_2$ $C_3 + C_3$	DMF/o-DCB (1/1)	Piperidine d-MA	180 °C /3 d	963 $m^2 g^{-1}$ 1036 $m^2 g^{-1}$ 1231 $m^2 g^{-1}$	2020	100
TM-TPT-COF	$C_3 + C_3$	o-DCB/*n*-BuOH (3/7)	NaOEt (s)	120 °C /3 d	810 $m^2 g^{-1}$	2020	103
PT-BN PB-BN	$C_3 + C_3$	DMF	Piperidine	170 °C /3 d	1150 $m^2 g^{-1}$ 968 $m^2 g^{-1}$	2020	114
g-$C_{30}N_6$-COF g-$C_{48}N_6$-COF	$C_3 + C_3$	o-DCB/*n*-BuOH (3/7)	KOH (s)	120 °C /3 d 150 °C /3 d	784 $m^2 g^{-1}$ 830 $m^2 g^{-1}$	2020	126
TAT-COF TPB-COF (g-$C_{33}N_3$-COF)	$C_3 + C_3$	MeOH/mesitylene (1/1)	NaOH (s)	180 °C /4 d	91 $m^2 g^{-1}$ 703 $m^2 g^{-1}$	2020	128

[a] o-DCB: o-dichlorobenzene; DMAc: Dimethylacetamide; DMF: *N,N*-Dimethylformamide; d-MA: Dimethylamine; TBAH: Tetrabutylammonium hydroxide; DBU: 1,8-Diazabicyclo[5.4.0]undec-7-ene; TFA: Trifluoroacetic acid.
[b] COFs made by the topology-templated synthesis in the presence of imine-linked COF analogs as templates.
[c] COFs made by Aldol condensation.
[d] COFs made by a one-pot reaction that combines cyclotrimerization of CH_3CN and subsequent Aldol condensation.
[e] COFs made by Horner-Wadsworth-Emmons reaction.

Please do not adjust margins

ARTICLE

2.3. Advantages of sp²c-COFs over other prototypical COFs

A diverse array of COFs with linkages ranging from boron-based linkages such as boroxine, boronate ester, borazine, and spiroborate , nitrogen-based linkages such as imine, β-ketoenamine, azine, hydrazone, imide, triazine, squaraine, imidazole, urea, aminal, phenazine, and pyrimidazole, to other robust linkages such as aryl ether and benzofuran have been reported to date.[51] As an emerging class of novel COFs, sp²c-COFs are advantageous due to their unparalleled combination of structural features as follows:

(1) Chemical stability. In contrast to dynamic linkages such as boron-based linkages and most nitrogen-based linkages that are vulnerable against aggressive chemicals, sp² C=C linkages with limited reversibility are chemically nonlabile, thereby leading to extraordinary chemical stability in various media including air, light, acidic, alkaline, and redox environments. The exceptional chemical stability not only allows for postsynthetic modification (PSM) of sp²c-COFs under extreme conditions but also underpins their superior performance over common COFs in applications under stringent conditions.

(2) High crystallinity. sp²c-COFs bypass the common crystallinity-stability dichotomy in COF chemistry and possess remarkable crystallinity. By comparison, chemically robust COFs such as covalent triazine frameworks,[52] and phenazine-linked COFs display limited crystallinity.[53]

(3) Structural complexity. The expansive library of monomers depicted in Fig. 1B coupled with the reticular synthesis has resulted in a rapidly increasing number of sp²c-COFs (> 40 in total) since 2016. In contrast, robust COFs bearing linkages such as imide,[54] aryl ether,[16] phenazine,[17] benzoxazole,[26] and imidazole[55] have significantly fewer reported structures, even some were developed prior to the emergence of sp²c-COFs. This is presumably due to the crystallization issue in *de novo* synthesis or reliance upon specialty linkers.

(4) π-electron delocalization. The intra-sheet π-electron delocalization over the 2D COF lattice is interrupted by non-conjugated (e.g., boron-based linkages) or polar linkage like imine, thus compromising their performance in optoelectronic applications. By contrast, the fully conjugated backbone of sp²c-COFs exhibits uninterrupted π-electron delocalization along the 2D lattice, which facilitates the migration, transfer, and transport of photons, holes, spins, and electrons, rendering them highly appealing in optoelectronics, spintronics, and energy storage.[56] Jiang's group demonstrated that sp²c-COF showed a redshift in UV-Vis absorption relative to its imine-linked COF analog,[31] validating that the sp² C=C linkage is superior to the C=N bond in terms of transmission of π-electrons over the lattice.

(5) Photoluminescence. Developing emissive and stable COFs has been a central topic in sensing applications.[57] However, most imine-linked 2D COFs are none or weakly luminescent, largely due to fluorescence quenching processes originating from π-π stacking interactions along with rotationally labile imine linkages.[58] Very limited emissive imine-linked 2D COFs have been made by incorporating chromophore struts such as pyrene or dehydrobenzoannulene into 2D polygons.[59-61] In contrast, sp² C=C linkages readily merge photoluminescence and stability to produce a variety of robust light-emitting 2D COFs. To name a few, an unsubstituted sp²c-COF (COF-1, aka g-$C_{18}N_3$-COF) presents a strong greenish-blue emission with a remarkable photoluminescence quantum yield (PLQY) of 25% whereas its imine-linked COF analog (COF-LZU1) is nonluminescent;[62] An isoreticular family of cyano-substituted sp²c-COFs (sp²c-COF, sp²c-COF-2, and sp²c-COF-3) emit strongly at 622, 606, and 609 nm, respectively.[63] Notably, the emissive properties of sp²c-COFs are well retained even after 1-year exposure to air while imine-linked COFs lost inherent properties. Most recently, a cyano-substituted sp²c-COF (2D CCP-2) displays the highest PLQY of 32.3 % among the 2D conjugated polymers and COFs.[64] The emissive sp²c-COFs with exceptionally high PLQY and durable photophysical properties present immense potential in various applications pertaining to lighting, bioimaging, and chemosensing.

Despite these notable advantages, sp²c-COFs are comparatively underexplored in comparison to other prototypical COFs such as imine-linked COFs, which were developed in 2009 and constituted the largest family of COFs nowadays.[65] Hence, sp²c-COFs possess relatively insufficient structural complexity and limited synthetic methodologies, which calls for more scientific attention to diversify the sp²c-COF library and advance their use in diverse applications.

2.4 Mechanistic insights into the formation of sp²c-COFs

The underlying mechanistic understanding of the crystallization pathway that governs COF formation and consequent properties is of utmost importance for the predictive synthesis of COFs.[66] Previous mechanistic investigations were merely limited to boronate ester- and imine-linked 2D COFs. In 2016, Dichtel's group revealed that imine-linked 2D COF was formed through a disorder-to-crystalline transition in which an amorphous polymer was formed quickly in the early stage and reconstructed into a crystalline material gradually.[67] They recently (2020) revised the mechanism and demonstrated that imine-linked 2D COFs formed as crystalline sheets in an extremely short time (~1 min) and rearranged into networks with more 3D order.[68] Up to now, the mechanistic study of sp²c-COF formation remains largely elusive and far lags behind the rapid development of new sp²c-COFs.

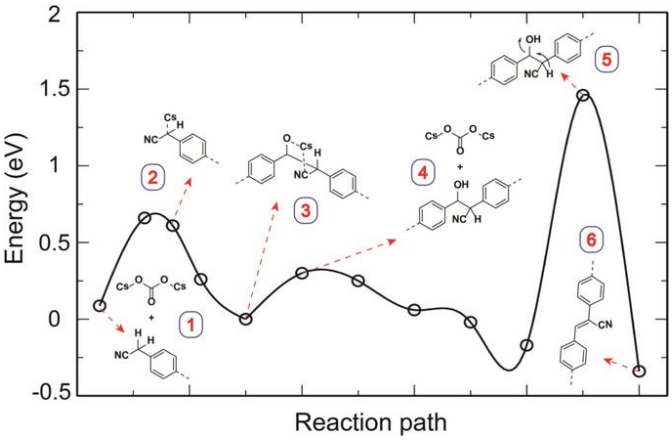

Fig. 2. Energy profiles at different stages (1-6) calculated using the DFT-NEB method describing the proposed reaction mechanism of the Knoevenagel condensation with Cs_2CO_3 as a catalyst. Reproduced from ref. 71 with permission from Wiley-VCH, copyright 2019.

Knoevenagel condensation, the most prominent reaction for the synthesis of sp^{2}c-COFs, exhibits dynamic characteristics under thermodynamic control. For instance, Lehn's group demonstrated the dynamic cross-Knoevenagel C=C/C=C exchange catalyzed by secondary amines such as L-proline.[69] Later, a dynamic covalent C=C/C=N exchange between the Knoevenagel compound and imine was revealed under catalyst-free conditions.[70] In light of the dynamic nature, the formation of sp^{2}c-COFs is prone to undergo the classic error-correcting and defect-healing process via thermodynamic equilibria. In 2019, Feng's group provided the first mechanistic insight into the pivotal role of catalytic Cs_2CO_3 in the synthesis of cyano-substituted sp^{2}c-COFs (i.e., 2D-CN-PPVs) via Knoevenagel condensation.[71] By using density functional theory (DFT)-nudged elastic band (NEB) calculations, they found that Cs_2CO_3 can effectively lower the energy barrier towards the initial C-C bond from stage 1 to stage 3 (Fig. 2), far surpassing other base catalysts. Through forming a five-membered transition state by bridging oxygen and nitrogen, Cs^+ facilitates a "quasi-reversible" C-C bond formation that is essential for achieving crystalline networks. Likewise, they recently (2020) used DFT calculations to map out the energy profile of the Horner-Wadsworth-Emmons (HWE) reaction in the presence of Cs_2CO_3, which aids the formation of unsubstituted sp^{2}c-COFs (CCP-Th and CCP-BD).[72] The energy profile indicates that Cs^+ forms a six-membered cyclic transition state to induce the reversible C-C formation in the HWE reaction, which is key to achieving the crystalline COFs.

Given the limited mechanistic studies that only focused on Cs^+-catalyzed formation of sp^{2}c-COFs, we envisage that more elaborate and broadly applicable investigations such as scrambling experiments,[73] kinetic studies,[74] *in-situ* X-ray diffraction analysis,[75] and computational simulation[76] are demanded to elucidate the crystallization process of sp^{2}c-COFs catalyzed by other catalysts beyond Cs_2CO_3.

3. Applications of sp^2 carbon-conjugated COFs

By merging a set of structural uniqueness such as well-ordered structures, amenable pore metrics, extended π-conjugated skeletons, permeant porosity, and outstanding chemical stability into one material, sp^{2}c-COFs have been broadly exploited in various applications. In this section, we will summarize the progress in the multifunctional applications of sp^{2}c-COFs and underscore their advantages by comparison with the imine-linked COF analogs and other reported systems.

3.1 Photocatalysis

Photocatalysis, which enables the direct solar-to-chemical conversion, has gained considerable attention in modern catalysis.[77] Among numerous heterogeneous photocatalysts such as inorganic semiconductors,[78] metal-organic frameworks (MOFs),[79] and π-conjugated polymers,[80] COFs stand out as extraordinary candidates due to their inherent regularity, permanent porosity, eco-friendly characteristic, tunable light harvesting, accessible open 1D channels, and high photostability. Consequently, enormous efforts have been directed to the development of COF-based photocatalysts.[81] Compared with conventional imine-, hydrazone-, or azine-linked COFs, which have limited capability of exciton migration and insufficient chemical robustness, sp^{2}c-COFs demonstrate strong light-harvesting, enhanced charge carrier mobilities over 2D lattices, and superior photostability, which are detrimental to the high efficiency of photocatalysis. This unique set of features empower sp^{2}c-COFs as emerging heterogeneous photocatalysts in a range of photocatalysis such as photocatalytic water splitting, CO_2 reduction, nicotinamide adenine dinucleotide phosphate (NADH) regeneration, degradation of organic pollutants, oxidation of arylamines, hydroxylation of arylboronic acids, and C-H trifluoromethylation of arenes (Table 2).

Table 2. The summary of the photocatalytic performance of sp^{2}c-COFs in diverse photocatalysis. [a]

sp^{2}c-COFs	Light irradiation	Photocatalysis	Co-catalyst	Sacrificial agent	Solvent	Activity	Ref.
sp^{2}c-COF	> 420 nm	Photocatalytic H_2 evolution	Pt	TEOA (10 vol %)	Water	1360 mmol h^{-1} g^{-1}	84
g-$C_{40}N_3$-COF g-$C_{31}N_3$-COF g-$C_{37}N_3$-COF	> 420 nm	Photocatalytic H_2 evolution	Pt	/	Water	4120 μmol $h^{-1}g^{-1}$ 542 μmol $h^{-1}g^{-1}$ 396 μmol $h^{-1}g^{-1}$	85
g-$C_{18}N_3$-COF g-$C_{33}N_3$-COF	> 420 nm	Photocatalytic H_2 evolution	Pt	TEOA (10 vol %)	Water	292 μmol $h^{-1}g^{-1}$ 74 μmol $h^{-1}g^{-1}$	88
g-$C_{54}N_6$-COF g-$C_{52}N_6$-COF	> 420 nm	Photocatalytic H_2 evolution	Pt	TEOA (10 vol %)	Water	2519 μmol $h^{-1}g^{-1}$ 1172 μmol $h^{-1}g^{-1}$	89
CCP-Th CCP-BD	> 420 nm	Photoelectrochemical water reduction	/	/	0.1M Na_2SO_4	7.9 μA cm^{-2} at 0 V	90
COF-alkene (2DPPV)	> 420 nm	Photocatalytic H_2 evolution	Pt	TEOA (20 vol %)	Water	2330 μmol h^{-1} g^{-1}	91
Bpy-sp^{2}c-COF	> 420 nm	Photocatalytic CO_2 reduction	$[Re(CO)_3Cl]$	/	0.1M Na_2SO_4	1040 mmol g^{-1} h^{-1} for CO with 81% selectivity	93

Please do not adjust margins

Bpy-sp^{2}c-COF	> 420 nm	Photocatalytic CO_2 reduction	$CoCl_2$	/	Water	17.93 mmol g^{-1} h^{-1} for CO with 81% selectivity	94
Por-sp^{2}c-COF	> 420 nm	Photocatalytic oxidation of secondary amines	/	/	CH_3CN	99% 0.5 h, RT	96
Por-sp^{2}c-COF	623 ± 8 nm	Photocatalytic oxidation of arylamines	TEMPO	/	CH_3CN	90-98% 15-30 min, RT	97
Py-BSZ-COF	520 nm	1. Photocatalytic oxidative amine coupling 2. thioamide cyclization	/	/	CH_3CN	1. 99% in 12-24 h, RT 2. 56-91% in 12-48 h, RT	98
TP-COF	420 nm	Photocatalytic NADH regeneration	/	/	Phosphate buffer	90.4% within 10 min, RT	99
TTO-COF (TM-TPT-COF)	≥ 420 nm	1. Photocatalytic degradation of dyes 2. C-H trifluoromethylation of arenes	/	/	1. Water 2. DMSO	1. >99% in 20 min, RT 2. 98% in 16 h, RT	48
COF-p-3Ph COF-p-2Ph COF-m-3Ph	> 420 nm	Photocatalytic hydroxylation of arylboronic acids	/	Triethylamine	CH_3CN	99%, 74%, 60% in 4 h, RT	100

[a] TEOA: triethanolamine; TMPO: 2,2,6,6-Tetramethylpiperidin-1-yl)oxyl; NADH: nicotinamide adenine dinucleotide phosphate; DMSO: Dimethyl sulfoxide; CH_3CN: acetonitrile; RT: room temperature.

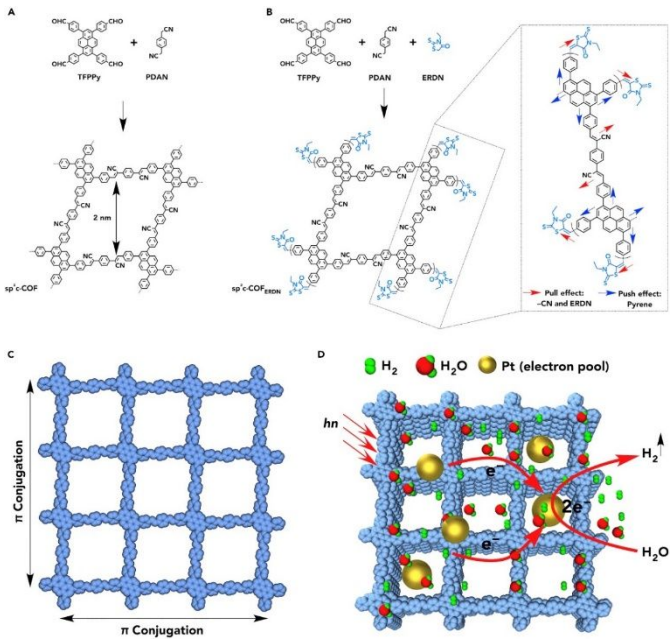

Fig. 3. Scheme of sp^{2}c-COFs for photocatalytic H_2 evolution reaction. A. The synthesis of sp^{2}c-COF by Knoevenagel condensation. B. The synthesis of sp^{2}c-COF$_{ERDN}$ with electron-deficient ERDN end groups. Inset: electron donor-acceptor pull-push effects on the 2D skeletons. C. Reconstructed crystalline 2D layer of sp^{2}c-COF that allows the π conjugation along x and y directions. D. Assembled light-driven interlocked system for H_2 production from water based on a sp^{2}c-COF and Pt water-reduction centers. Reprinted from ref.84 with permission from Elsevier, copyright 2018.

Photocatalytic hydrogen evolution reaction (HER), which turns solar energy into H_2 from water, is recognized as a sustainable route to H_2, an essential alternative clean energy to address the pressing energy demand in the post-carbon future. Since the first COF photocatalyst for HER in 2014,[82] considerable endeavors have been devoted to applying COFs for efficient H_2 production from water.[83] In 2018, Jiang's group developed a cyano-substituted sp^{2}c-COF by Knoevenagel condensation between tetrakis(4-formylphenyl) pyrene and 1,4-phenylenediacetonitrile (PDAN),[84] and the obtained COF was utilized in photocatalytic HER for the first time (Fig. 3A). The unique combination of π-conjugation, crystallinity, porosity, and photostability enabled sp^{2}c-COFs to harvest a broad range of light and produce a steady H_2 evolution rate of 1360 mmol $h^{-1}g^{-1}$ from water. To further enhance the light absorbance and narrow the bandgap, they integrated the electron-deficient 3-ethylrhodanine (ERDN) motif into the sp^{2}c-COF to afford donor-acceptor heterojunction (sp^{2}c-COF$_{ERDN,}$ Fig. 3B). Consequently, sp^{2}c-COF$_{ERDN}$ showed dramatically boosted photocatalytic activity with striking high H_2 evolution rates of 2120 and 1240 mmol $h^{-1}g^{-1}$ upon light irradiation at wavelengths of 420 and 498 nm, respectively, which far exceeded those of the pristine sp^{2}c-COF, amorphous counterpart, other common COFs and state-of-the-art systems such as graphitic carbon nitride (g-C_3N_4). Notably, the imine-linked COF counterpart was completely inactive under identical conditions, underscoring the advantages of sp^{2}c-COFs in photocatalytic HER.

Not only cyano-substituted sp^{2}c-COFs but also unsubstituted sp^{2}c-COFs showed remarkable activity in photocatalytic HER. In 2019, Zhang's group reticulated 3,5-dicyano-2,4,6-trimethylpyridine with 4,4″-diformyl-p-terphenyl, 4,4′-diformyl-1,1′-biphenyl (DFBP) and 1,3,5-tris(4-formylphenyl) benzene (TFPB) to afford three unsubstituted sp^{2}c-COFs (g-$C_{40}N_3$-COF, g-$C_{31}N_3$-COF, and g-$C_{37}N_3$-COF, respectively).[85] The high surface area (up to 1235 m^2g^{-1}), ordered structures, and well-aligned band energy levels rendered g-$C_{40}N_3$-COF as a promising catalyst for visible-light-driven HER. In the presence of platinum (Pt) co-catalyst, g-$C_{40}N_3$-COF displayed a high H_2 production rate of 4120 μmol $h^{-1}g^{-1}$ at a wavelength of 420 nm, with a remarkable apparent quantum efficiency (AQY) of 4.84%, exceeding the AQYs of most COF photocatalysts such as imine-linked N_3-COF,[86] hydrazone-linked TFPT COF,[82] and *β*-ketoenamine-linked

 This journal is © The Royal Society of Chemistry 20xx

Please do not adjust margins

FS-COFs.[87] DFT calculations on the free-energy changes revealed that the pyridine-nitrogen in g-$C_{40}N_3$-COF acts as the primary active site for HER, Likewise, two triazine-cored unsubstituted sp^2c-COFs (g-$C_{18}N_3$-COF and g-$C_{33}N_3$-COF) were developed via Knoevenagel condensation of 2,4,6-trimethyl-1,3,5-triazine (TMTA) with ditopic 1,4-diformylbenzene and tritopic TFPB, respectively.[88] Noteworthy, g-$C_{18}N_3$-COF film, obtained by *in situ* growth on indium tin oxide, showed a high photocurrent of up to 45 μA cm^{-2} at 0.2 V vs reversible hydrogen electrode (RHE) and rapid interfacial charge transfer. Upon visible light irradiation, Pt-modified g-$C_{18}N_3$-COF exhibited a H_2 production rate of 292 μmol $h^{-1}g^{-1}$ with an AQY of 1.06% at 420 nm, which is significantly higher than that of its imine-linked COF analog, which nearly lost its crystallinity upon 4 hour light exposure, indicating the superior photostability of sp^2c-COFs over their imine-linked COF counterparts.

The polarity of sp^2c-COFs can profoundly influence their semiconducting properties and subsequent photocatalytic performance. For example, two unsubstituted sp^2c-COFs (g-$C_{54}N_6$-COF and g-$C_{52}N_6$-COF) with tuned polarity were recently developed by reticulating 2,4,6-tris (4′-formyl-biphenyl-4-yl)-1,3,5-triazine with D_{3h}-symmetric tricyanomesitylene and C_{2v}-symmetric 3,5-dicyano-2,4,6-trimethylpyridine, respectively.[89] The octupolar π-conjugated g-$C_{54}N_6$-COF exhibited enhanced light harvesting as well as photo-induced charge generation and separation relative to g-$C_{52}N_6$-COF. Due to these distinguishing features, g-$C_{54}N_6$-COF robustly produced H_2 at a rate of 2518.9 mmol h^{-1} g^{-1} that was among the highest values of COF-based photocatalysts. Besides HER, g-$C_{54}N_6$-COF displayed one of the highest photocatalytic O_2 evolution rate (51 mmol h^{-1} g^{-1}) among COF systems, indicating the immense prospect of sp^2c-COFs for spontaneous photocatalytic water splitting into H_2 and O_2. Moreover, g-$C_{54}N_6$-COF showed significantly higher photocatalytic performance than that of the less-symmetric g-$C_{52}N_6$-COF, implying that altering the geometric symmetry of monomers within sp^2c-COFs could exert a profound effect on their photocatalytic performance.

In addition to photocatalytic water splitting,[90-91] photocatalytic conversion of CO_2 into value-added hydrocarbons has been a continuous hot topic in clean energy research.[92] In 2019, Chen, Sprick, Cooper, and co-workers encapsulated a molecular rhenium complex, [Re(bpy)$(CO)_3$Cl], into a 2,2′-bipyridine-containing sp^2c-COF to fabricate a heterogeneous photocatalyst (Re-Bpy-sp^2c-COF).[93] Due to the strong visible-light absorption up to 694 nm, high CO_2 binding affinity, and exceptional photostability, Re-Bpy-sp^2c-COF gave a high CO production rate of 1040 mmol g^{-1} h^{-1} with an 81% CO/H_2 selectivity under 17.5 hours visible-light irradiation, substantially outperforming its homogeneous Re counterpart. Furthermore, upon the addition of a photosensitizer, Re-Bpy-sp^2c-COF showed an increased CO production rate up to 1400 mmol g^{-1} h^{-1} with an improved selectivity of 86%. Loading colloidal Pt nanoparticles into Re-Bpy-sp^2c-COF resulted in the co-formation of CO and H_2, whose composition can be well adjusted by varying the amount of loaded Pt. Moreover, the amorphous counterpart was catalytically inactive, suggesting that the structural regularity of COFs is essential to the effective CO_2 reduction. Replacing the Re with earth-abundant cobalt complex in Bpy-sp^2c-COF (sp^2c-COF_{dpy}-Co) lead to a CO production at 17.93 mmol g^{-1} with an 81.4% CO/H_2 selectivity,[94] placing it among the highest performing non-noble-metal COF catalyst in photocatalytic CO_2 reduction. Theoretical calculations coupled with *in situ* transient techniques revealed that the facile intramolecular electron delivery via electron cascade in the sp^2c-COF contributed to the high efficiency in CO_2 photoreduction.

Photoredox organic transformation provides a viable means to fine chemicals with minimal side products, low-energy consumption, and eco-friendly characteristics. The exploration of COF photocatalysts has evoked substantial interest recently.[95] In 2019, the first porphyrin-based cyano-substituted sp^2c-COF (Por-sp^2c-COF) was derived from Knoevenagel condensation of C_4-symmetric 5,10,15,20-tetrakis(4-benzaldehyde) porphyrin and C_2-symmetric PDAN.[96] Por-sp^2c-COF was deployed as a heterogeneous photocatalyst for the visible-light-induced oxidation of secondary amines to imines, which remains a grand challenge for COFs carrying normal linkages owing to the presence of chemically aggressive arylamines. The robust sp^2 C=C linkages and enhanced π-conjugation endowed Por-sp^2c-COF with exceptional chemical stability toward high-concentration amines and superior photocatalytic activity over its imine-linked Por-COF counterpart, which was completely decomposed under identical conditions. Notably, Por-sp^2c-COF outperformed plenty of prior photocatalysts, such as g-C_3N_4, conjugated microporous polymers, and MOFs. In recent subsequent work (2020), Por-sp^2c-COF was combined with 2,2,6,6-tetramethylpiperidin-1-yl)oxidanyl (TEMPO) to afford a cooperative photocatalyst for the first red-light-induced oxidation of arylamines.[97] Por-sp^2c-COF showed high yields within just 30 minutes at room temperature in the oxidation of various substituted arylamines under red light illumination. Importantly, Por-sp^2c-COF was readily reusable in 3 consecutive photocatalytic runs whereas its imine-linked Por-COF analog failed to survive under the same conditions, clearly highlighting the advantages of sp^2c-COFs over traditional COFs in photocatalysis that involves harsh conditions.[98]

The first triazine-based sp^2c-COF (TP-COF) was prepared through Knoevenagel condensation of 2,4,6-tris(4-formylphenyl)-1,3,5-triazine (TFPT) and PDAN in 2019.[99] The improved chemical stability and π-conjugation endowed by sp^2 C=C linkages, together with the tailorable semiconducting properties from triazine cores, make TP-COF a promising artificial photosystem I (PSI). For the first time, TP-COF was used to catalyze the coenzyme regeneration wherein a-ketoglutarate was converted to L-glutamate under visible-light illumination. Remarkably, TP-COF exhibited a record-high yield of 97% in only 12 minutes, rendering it the highest-performing artificial PSI. Just recently, a series of isoreticular unsubstituted sp^2c-COFs (COF-p-3Ph, COF-p-2Ph, and COF-m-3Ph) were derived by coupling tricyanomesitylene with C_2- or C_3-symmetric aryl aldehydes catalyzed by organic bases at 180 °C.[100] The resultant COFs possessed high surface areas (up to 1231 m^2 g^{-1}), superb π-conjugation, broad light harvesting, and tunable bandgaps. Consequently, sp^2c-COFs efficiently catalyzed the visible-light-induced aerobic oxidation of various aryl boronic acids with excellent yields at room temperature, significantly outperforming the corresponding amorphous analogs, g-C_3N_4, and previously reported benzoxazole-linked COF photocatalyst (LZU-190). Remarkably, COF-p-3Ph can be reused for at least 10 catalytic cycles without apparent decay in both activity and crystallinity. Along this line, a triazine-based unsubstituted sp^2c-COF (TTO-COF) was constructed by a trifluoroacetic acid-catalyzed Aldol condensation between TMTA and TFPT.[48] Thanks to the sp^2 C=C linkage, TTO-COF showed high chemical stability under harsh conditions and broad light absorption with an optical bandgap of 2.46 eV. These unique features enabled TTO-COF to catalyze the photocatalytic degradation of organic dyes in aqueous medium and C-H functionalization of aromatic substrates with high yields and good reusability up to 3 cycles, which outperformed g-C_3N_4 and its imine-linked COF counterpart.

Despite the promising progress of sp^2c-COFs in photocatalysis, the exploration of sp^2c-COF photocatalyst is still in the nascent stages and merits further efforts. Therefore, it is necessary to extend the applicability of sp^2c-COFs to a range of sought-after photocatalytic

Please do not adjust margins

applications. On the other hand, an in-depth molecular-level mechanistic insight into the underlying photocatalytic processes is of prime significance but remains elusive. Hence, fundamental understandings are called for to elucidate the complex reaction pathway and guide the rational design of COF photocatalysts.[101]

3.2 Other catalysis

Aside from photocatalysis which dominates the catalytic applications of sp^2c-COFs, they have also been exploited in conventional heterogeneous organocatalysis and electrocatalysis. However, the relevant study is still in its infancy and deserves further research efforts.[102]

The first unsubstituted sp^2c-COF (COF-701) was reported by Yaghi's group in 2019 through Aldol condensation between TMTA and DFBP using trifluoroacetic acid as a catalyst.[47] COF-701 adopted a unique staggered conformation and the largest Brunauer-Emmett-Teller (BET) surface area of 1366 m^2 g^{-1} among all the established sp^2c-COFs. The unsubstituted sp^2 C=C linkage endowed COF-701 with outstanding chemical stability toward acid, base, and organolithium reagents. To highlight the stability and advance the use of sp^2c-COF in heterogeneous catalysis, they immobilized a strong Lewis acid, $BF_3{\cdot}OEt_2$ into COF-701 to afford a rare acidic COF catalyst. The obtained BF_3@COF-701 not only retained inherent primary structure but showed high activity in a Diels-Alder reaction.

In addition to the benchmark Lewis-acid organocatalysis, sp^2c-COF has been explored as an efficient electrocatalyst with outstanding performance. Most recently (2020), a triazine-cored unsubstituted sp^2c-COF (TM-TPT-COF, aka TTO-COF) was developed by Knoevenagel condensation of TMTA and TFPT catalyzed by EtONa.[103] TM-TPT-COF served as a promising scaffold for hosting Pt nanoparticles due to its high stability, ordered micropores, nitrogen-rich pore interiors, and large BET surface area. Upon the facile reduction with methanol, ultrasmall Pt nanoparticles with an average size of 2.1 nm were uniformly distributed throughout the COF (Pt@COF) without compromising the inherent properties of the host. Notably, Pt@COF demonstrated high activity in the electrocatalytic oxygen reduction reaction (ORR) in an acid media with an onset potential of 1.05 V versus RHE and a half-wave potential of 0.89 V, which outperformed the commercial Pt/carbon and prior reported Pt-based electrocatalysts. The excellent ORR performance was rationalized by the synergistic effects of robust triazine-based skeletons, enhanced electron transfer, ordered porous structures, and highly accessible ultrasmall Pt nanoparticles. This work unlocks the vast potential of sp^2c-COFs in electrocatalysis such as ORR and will trigger more consideration in other catalytic transformations.[104]

3.3 Radionuclides sequestration

Water pollution has evolved into a global crisis that jeopardizes public health. Among the various contaminants, radionuclides raised substantial concerns due to the ever-increasing use of nuclear power and improperly disposed nuclear wastes in the aquatic environment, which spurred significant efforts toward radionuclides sequestration. Compared with existing remediation methodologies, adsorptive removal has been deemed as environmentally benign, easy-to-operate, energy-efficient, and cost-effective.[105] Adsorbent materials with a set of unique features including high binding affinity, rapid kinetics, selectivity, stability, and large capacity are highly demanded yet represent a grand challenge. Unlike developed adsorbents such as activated carbons, zeolites, MOFs, and porous organic polymers, COFs hold great promise for radionuclides sequestration from water owing to the lightweight characteristic, periodic structures, high surface areas, modular functionalities, and accessible chelating sites.[106] However, poor chemical stability rooted in dynamic linkages severely restricted their broad use in real life radionuclides sequestration.[107]

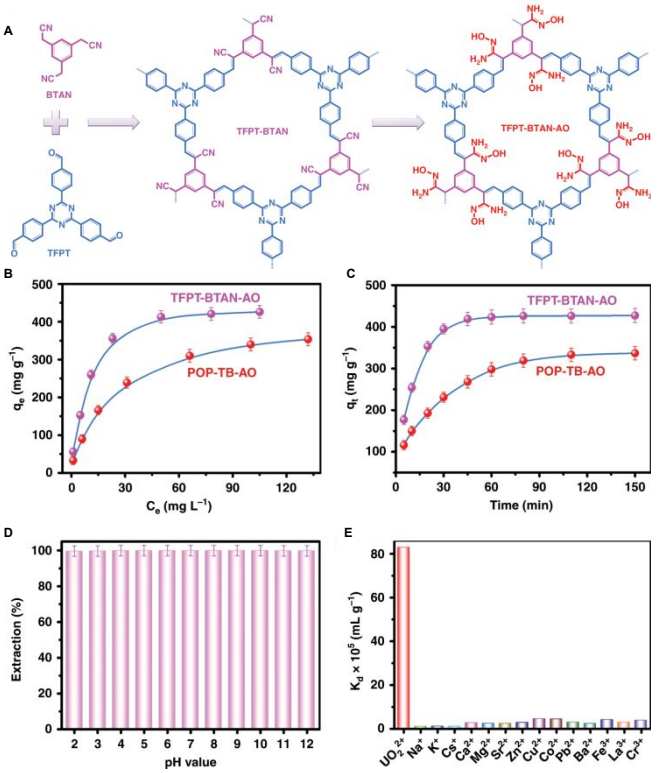

Fig. 4 A. Synthesis of amidoxime-tagged TFPT-BTAN-AO via PSM of TFPT-BTAN. B. Adsorption isotherm of UO_2^{2+} for TFPT-BTAN-AO and amorphous POP-TB-AO at pH 4. C. Adsorption kinetics of UO_2^{2+} for TFPT-BTAN-AO and amorphous POP-TB-AO at pH 4. D. The extraction efficiency of UO_2^{2+} at different pH. E. The selective adsorption of the test metal ions. Reprinted from ref.108 with permission from Springer Nature, copyright 2020.

To address this issue, Qiu and co-workers firstly developed a stable and emissive amidoxime-tagged sp^2c-COF (TFPT-BTAN-AO) for simultaneous uranium detection and removal from water. TFPT-BTAN-AO was constructed by Knoevenagel condensation of TFPT and 2,2′,2″-(benzene-1,3,5-triyl)triacetonitrile (BTAN), followed by the conversion of pendant cyano groups to amidoxime moieties, which are well known for the efficient uranium chelation (Fig. 4A).[108] The emissive TFPT-BTAN-AO exhibited ultrahigh sensitivity toward uranyl ions (UO_2^{2+}) as low as 6.7 nM via a fluorescence quenching mechanism. Moreover, the abundant and highly accessible amidoxime adsorption sites arranged in the regular 1D nanochannels enabled the use of TFPT-BTAN-AO as a solid extractor with a high uranium uptake capacity of 427 mg g^{-1} and fast adsorption kinetics, significantly outperforming the amidoxime-free TFPT-BTAN, amorphous analogs (Figs. 4B and 4C), and previously reported COF adsorbents such as *β*-ketoenamine-linked COF-TpDb-AO,[109] and azine-linked ACOF.[110] Notably, the robust sp^2 C=C linkage ensured a high uranium removal efficiency in a broad pH range of 2-12 (Fig. 4D), highlighting the ultrastability and prospect of TFPT-BTAN-AO in practical uranium mining. Moreover, the significantly higher distribution coefficient than the distinguishing standard underscored the superb affinity of TFPT-BTAN-AO toward UO_2^{2+} (Fig. 4E). Extending this strategy to other COFs, Qiu's group subsequently developed two new amidoxime-based sp^2c-COFs with varying

This journal is © The Royal Society of Chemistry 20xx

Please do not adjust margins

topologies and functionalities.[111] The triazine-cored hexagonal TP-COF-AO showed an exceptionally high uranium uptake capacity of 436 mg g^{-1}, rapid adsorption in just 10 minutes, and excellent reusability for at least 8 cycles. The other tetragonal COF-PDAN-AO,[112] obtained by stepwise PSM of COF-PDAN (aka sp^2c-COF in Fig. 3), also exhibited extremely high sensitivity toward UO_2^{2+} as low as 6.5 nM, even in the presence of competing metal ions. Moreover, COF-PDAN-AO was highly recyclable and showed a high uranium uptake capacity of 410 mg g^{-1} even in an acidic media at pH 4.

To further augment the uranium sequestration, photo-enhanced extraction emerged as a promising and feasible approach recently. For example, two optoelectronically active amidoxime-tagged sp^2c-COFs were applied for photo-enhanced uranium extraction from seawater. The COFs (NDA-TN-AO and BDA-TN-AO) were constructed by condensing 2,2′,2″-(benzene-1,3,5-triyl)triacetonitrile (TN) with naphthalene-2,6-dicarbaldehyde (NDA) or 4,4′-biphenyldicarboxaldehyde (BDA), respectively.[113] Subsequently, the inborn cyano groups were converted to uranyl chelating amidoxime moieties. Owing to the fully conjugated 2D backbones and excellent semiconducting properties, NDA-TN-AO exhibited high antibacterial activity and excellent photo-reduction of U^{VI} to U^{IV}. Further, upon the illumination of simulated sunlight, NDA-TN-AO showed a drastically enhanced uranium uptake capacity from 486.4 to 589.1 mg g^{-1}, positioning it as the highest-performing uranium adsorbents. They attributed the boosted adsorption to the positive surface charge of NDA-TN-AO induced by the photoelectric effect to electrostatically attract $[UO_2(CO_3)_3]^{4-}$, which allowed the NDA-TN-AO to extract uranium at a capacity of 6.07 mg g^{-1} in natural seawater under light illumination. Moreover, the ultrastable NDATN-AO adsorbent can be fully recycled for 6 consecutive runs and the adsorption capacity increased after 27-day light irradiation, highlighting the exceptionally high long-term stability. Encouraged by the initial success, three new amidoxime-based sp^2c-COFs (PT-BN-AO, BD-TN-AO, and ED-TN-AO) were analogously achieved by the PSM of cyano-containing sp^2c-COFs recently.[114-115] The consequent superb anti-biofouling activity and photoelectric effect enabled a much higher uranium extraction capacity in natural seawater than that without light irradiation.

Amidoxime-based sp^2c-COFs represent an emerging paradigm for simultaneous uranium detection and sequestration with high selectivity, capacity, rapid kinetics, and good reusability, unleashing the enormous potential of sp^2c-COFs for practical uranium monitoring and removal from seawater. However, the current use of sp^2c-COFs in water remediation merely focused on uranium extraction. Hence, extending the applicability of sp^2c-COFs in the detection and subsequent extraction of other high-priority water contaminants such as heavy metal ions, volatile organic chemicals, perfluorinated compounds, and oil spills is of fundamental and practical interest.

3.4 Cathode in lithium-ion batteries

Lithium-ion batteries (LIBs) are the dominant energy storage technology nowadays in powering commercial electronics and electric vehicles due to their unparalleled combination of high energy and power density.[116] In a marked difference from inorganic cathodes that suffer from drawbacks including low energy density, safety hazards, and environmental pollution, organic cathodes provide an appealing alternative due to their unique features such as lightweight, environmental benignity, high theoretical capacity, structural tunability, and functional flexibility.[117] Among the wide array of organic polymer cathodes, COFs have emerged as promising organic cathode materials for LIBs due to the unique structural attributes.[118] Up to now, the exploration of COF cathodes mainly focused on imine-linked 2D COFs, whose insufficient electrochemical stability severely stunted their practical application in rechargeable batteries.

The first implementation of sp^2c-COF (CCP-HATN) as a high-performance organic cathode for LIBs was demonstrated by Feng's group in 2018.[119] CCP-HATN was synthesized by linking 2,3,8,9,14,15-hexa(4-formylphenyl) diquinoxalino[2,3-a:2′,3′-c]phenazine (HATN-6CHO) with PDAN through Knoevenagel condensation (Fig. 5A). The sp^2 C=C linkages empowered CCP-HATN with exceptional chemical and electrochemical stabilities. CCP-HATN retained its crystallinity upon the exposure to aqueous HCl (12 M) and NaOH (12 M) while the imine-linked COF counterpart (2D C=N HATN) was decomposed. Apart from enhanced stability, CCP-HATN displayed superior redox properties over C=N HATN evidenced by the cyclic voltammetry curve. To further improve the electrical conductivity of pristine COF, CCP-HATN was grown *in situ* on the surface of carbon nanotubes (CNTs) with the retention of crystallinity (Fig. 5B). When implemented as an organic cathode for LIBs, the obtained CCP-HATN@CNT composite showed a high capacity of 94 mAh g^{-1} even at 1.0 A g^{-1}, outperforming most prior HATN-containing materials.[120-122] Moreover, it exhibited remarkable long-term cycling stability with 91% capacity retention after 1000 cycles (Fig. 5C). The high performance was presumably due to the high electrochemical stability of sp^2c-COF, core-shell nanostructure, and a surface-controlled pseudocapacitive process.

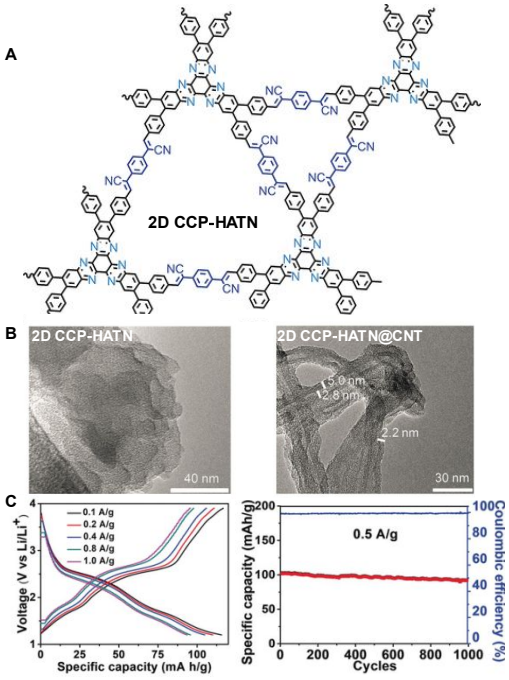

Fig. 5. A. Schematic illustration of 2D CCP-HATN; B. TEM images of 2D CCP-HATN and 2D CCP-HATN@CNT; C. Charge-discharge profiles of 2D CCP-HATN@CNT at different current densities and cycling performance of 2D CCP-HATN@CNT at 0.5 A g^{-1}. Adapted from ref. 119 with permission from Wiley-VCH, copyright 2019.

The use of sp^2c-COFs as electrodes remains largely unexplored relative to imine-linked COFs considering only one attempt made to date. We anticipate that leveraging the structural merits of sp^2c-COFs will pave a promising avenue to develop advanced organic electrodes for various alkali ion batteries such as LIBs, sodium-, and potassium-ion batteries.

3.5 Supercapacitors

Please do not adjust margins

Supercapacitors, one of the most vital electrical energy storage systems, are ubiquitously utilized in portable electronics and electric vehicles.[123] The increasing energy demand necessitates the development of high-performance supercapacitors with high capacitance, ultrafast charge-discharge rate, and long life cycle. COFs have emerged as an apt candidate for advanced supercapacitors, primarily due to their large surface areas, periodic skeletons, atomic-level tunability, and densely distributed redox-active motifs in regular channels of COFs.[124] For the fabrication of COF supercapacitors, there are typically two main strategies, that is, direct carbonation of COFs into porous carbons and doping COFs with electrically conducting additives.

sp^2c-COF-derived porous carbons (2DPPV-700-900) for supercapacitors were developed in 2016 by the pyrolysis of the first cyano-substituted sp^2c-COF (2DPPV) under an inert atmosphere at various temperatures (700, 800, and 900 °C). 2DPPV was prepared by Knoevenagel condensation of PDAN and TFPB using Cs_2CO_3 as a catalyst and possessed abundant pendant cyano groups in the ordered 2D lattice,[30] which enabled the formation of nitrogen-doped porous carbons with a high surface area of up to 880 m^2 g^{-1} upon pyrolysis. When used as supercapacitors, 2DPPV-800 exhibited a high specific capacitance of 334 Fg^{-1} at 0.5 Ag^{-1}, exceeding those of 2DPPV-700, 2DPPV-900, and most reported porous carbons. Notably, 2DPPV-800 had exceptionally high cycling stability without any capacitance loss even after 10000 cycles, revealing the great potential of using sp^2c-COF as template precursors toward 2D carbons for high-performance energy storage. However, the high-temperature pyrolysis destroys the long-range orders of COFs and leads to unforeseeable structural changes.

In addition to COF-derived carbons obtained via pyrolysis, sp^2c-COFs can be alternatively composited with electronically conductive materials for energy storage. In 2019, Zhang's group developed a new unsubstituted sp^2c-COF (g-$C_{34}N_6$-COF) by reacting 3,5-dicyano-2,4,6-trimethylpyridine with TFPT using piperidine as a catalyst (Fig. 6A).[125] g-$C_{34}N_6$-COF possessed ordered porous structure, triazine-based skeleton, unique nanofibrous morphology, and superb stability against aggressive chemicals. The freestanding g-$C_{34}N_6$-COF film was prepared by vacuum filtration with single-walled carbon nanotubes as conductive additives. The mechanically robust thin film enabled the first fabrication of COF-based interdigital micro-supercapacitors (MSC) through mask-assisted vacuum filtration. Remarkably, the obtained flexible COF-MSC showed high specific areal capacitances and excellent energy densities, outperforming most reported MSCs using different electrode materials such as graphene and phosphorene. In a recent follow-up study (2020), two new unsubstituted sp^2c-COFs were prepared by linking TMTA with tritopic triazine-cored aldehydes (g-$C_{30}N_6$-COF and g-$C_{48}N_6$-COF, Fig. 6B and 6C).[126] When doped with carbon nanotubes (CNTs), continuous and mechanically robust COF/CNT films were obtained via a stepwise vacuum filtration/hot-pressing process. The COF/CNT film was further fabricated into interdigital microelectrodes and assembled on polyethylene terephthalate substrate to afford flexible COF-MSCs, which exhibited a high areal capacitance and volumetric energy density, significantly exceeding those of the commercial energy storage devices and g-$C_{34}N_6$-COF-MSC. Further, both COF-MSCs showed excellent cycling stability and retained nearly 95% capacitance after 5000 charge/discharge cycles. These flexible, robust, and tailor-made sp^2c-COF-based MSCs open up numerous opportunities in the development of advanced portable electrical energy storage devices.

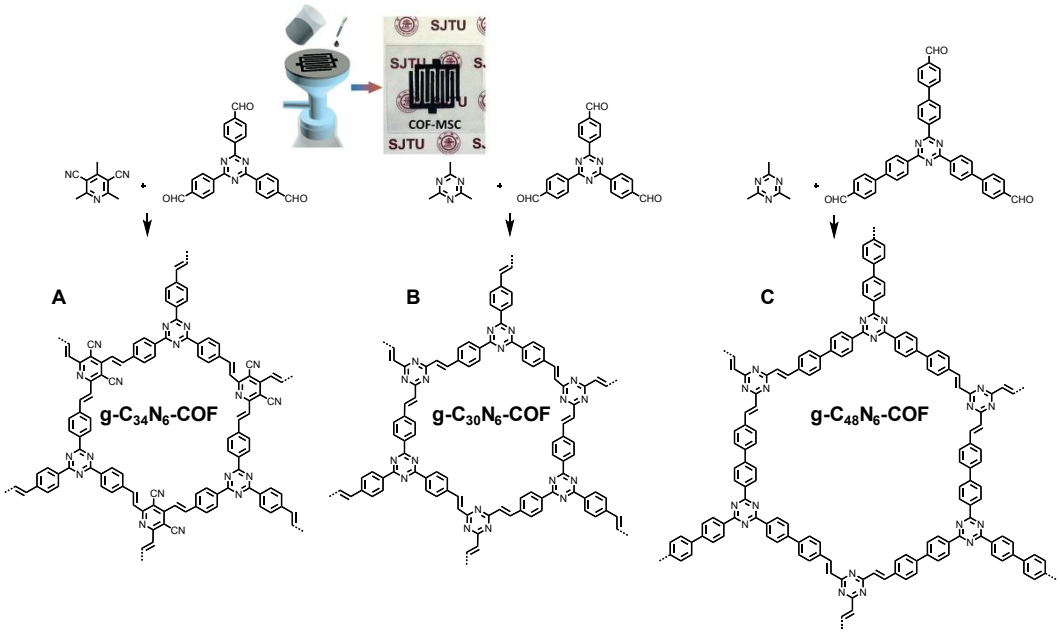

Fig. 6. The preparation of three isoreticular sp^2c-COF-MSC devices through vacuum filtration with a lab-made interdigital mask. Modified from ref. 125 with permission from Wiley-VCH, copyright 2019.

3.6 Optical applications

The highly emissive properties, together with the tailor-made architecture, exceptional photostability, and high surface area, endow sp^2c-COFs with vast potential in optical applications such as optoelectronic devices, information security protection, and chemosensors. Importantly, the atomic-level modularity of composition and topology renders sp^2c-COFs as an ideal platform to precisely tailor the optoelectronic properties and establish clear structure-property correlations, thereby offering fundamental principles for the rational design of tailor-made emissive COFs.

The first cyano-substituted sp^2c-COF, cyano-sp^2c-COF (aka 2DPPV) was recently (2020) found to display strong two-photon absorption and fluorescence owing to the extended sp^2 carbon-

This journal is © The Royal Society of Chemistry 20xx

Please do not adjust margins

conjugated backbone and intramolecular interaction.[127] In sharp contrast, its boronate ester- and imine-linked COF analogs had no or weak luminescence in the solid state. To explore its use in information encryption, cyano-sp^{2}c-COF was blended with polyvinylidene fluoride to afford a "security ink" to print the logo and badge of Sun Yat-sen University (SYSU), which were invisible under visible light. By illuminating with near-infrared (NIR) light, both logo and badge displayed yellow two-photon emission and thus can be distinguished (Fig. 7A). Further, they explored the use of cyano-sp^{2}c-COF in the design of white light-emitting diode (LED) devices, which emerged as a promising alternative to conventional light sources. They blended commercial green phosphor (*β*-Sialon: Eu^{2+}) with cyano-sp^{2}c-COF to regulate the commission on illumination (CIE) coordinates. Using a dip-coating method, a thin COF/green phosphor film was homogeneously coated onto a blue LED chip (Fig. 7B). The CIE coordinates and color rendering index of the COF-based LED device were well adjusted by altering the ratio of green phosphor and COF, giving rise to a high color rendering index and high luminous efficacy. The obtained CIE coordinates were fairly close to those of pure white light (Fig. 7C). Motivated by the enormous promise of sp^{2}c-COFs as efficient metal-free phosphors in the design of white LEDs, Huang's group recently developed two emissive unsubstituted sp^{2}c-COFs, TAT-COF and TAB-COF (aka g-$C_{33}N_3$-COF) with distinct monomer planarity for the fabrication of white LED devices, which were produced by a simple coating of COF films onto a cyan LED chip.[128] Furthermore, mixing two COFs with adjusted ratios lead to colors across the whole visible spectrum. Interestingly, TAT-COF, synthesized by reacting TMTA with a planar 2,7,12-triformyl-5,10,15-triethyltriindole (TAT), displayed broader absorption, slower transient absorption decay kinetics, stronger interlayer charge transfers than those of TPB-COF synthesized with a propeller-like monomer (TFPB). To gain an in-depth mechanistic insight, they resorted to a combination of time-resolved absorption/emission spectroscopy and computational simulation and demonstrated that the intrinsic structural parameters including backbone planarity, π-conjugation, dipole moment orientation, and interlayer aggregation play a crucial role in the exquisite control of the exciton relaxation pathway and PLQY of sp^{2}C-COFs, offering unprecedented fundamental guidance for the rational design of emissive sp^{2}c-COFs.

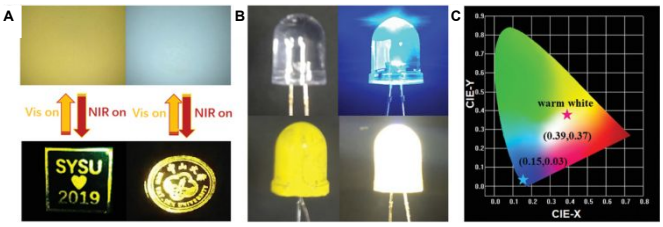

Fig. 7 Optical applications of cyano-sp^{2}c-COF. A. Photographs of the cyano-sp^{2}c-COF ink printed logo of SYSU 2019 and Sun Yat-sen University under visible light or NIR. B. Photograph of the LEDs: the pristine LED (turning off), the pristine LED (turning on and emitting blue light), the pristine LED coated with a thin coating layer (turning off), and the coated LED (turning on and emitting white light). C. A CIE-1931 chromaticity diagram and the positions (marked by the stars) for blue LED (0.15, 0.03) and warm white LED (0.39, 0.37). Reproduced from ref. 127 with permission from Wiley-VCH, copyright 2020.

Apart from the intriguing applications in designing white LEDs, sp^{2}c-COFs also show great promise as efficient sensors for detecting various substances. For instance, Jiang and co-workers demonstrated the use of an emissive cyano-substituted sp^{2}c-COF (Fig. 3A) in the ultrasensitive detection of Cu^{2+} ions (structure in Fig. 3A).[63] Upon the addition of Cu^{2+}, the fluorescence of sp^{2}c-COF in tetrahydrofuran was effectively quenched whereas the addition of Zn^{2+} that cannot bind to cyano groups was incapable of quenching the emission, suggesting the metal-cyano interaction was critical for triggering fluorescence sensing. Notably, sp^{2}c-COF displayed extremely high sensitivity to the Cu^{2+} ion with a striking ppb-level detection limit and an extremely high fluorescence quenching rate constant (4.1×10^{14} M^{-1} s^{-1}), indicating the exceptionally high selectivity and effectiveness of the sp^{2}c-COF sensor for detecting Cu^{2+} ions. Besides metal ions, chiral substrates detection is of immense importance in both academia and industry. Just recently, the first chiral crown ether-containing sp^{2}c-COFs (CCOF 17 and CCOF 18) were developed by Knoevenagel condensation of dibinaphthyl-22-crown-6-based tetrabenzaldehyde with PDAN and 4,4'-biphenyldiacetonitrile, respectively.[129] The robust sp^2 C=C linkages allowed for the successful crystal-to-crystal transformation via the direct reduction of C=C bonds. By virtue of the emissive properties, robust frameworks, and built-in chiral crown ether groups as recognition sites, CCCOFs was applied as enantioselective sensors and exhibited remarkable fluorescence recognition for three chiral amino alcohols with high enantioselectivity, outperforming their reduced COF counterparts, molecular analogs, and most previously reported chiral sensors.

Albeit the great promises, the potential of sp^{2}c-COFs as chemical sensors has not been fully unleashed. Exploring emissive sp^{2}c-COFs as smart sensors for detecting various in-demand substances such as gas, explosives, humidity, biomolecules, and metal ions is much desired.[57]

4. Conclusion and prospect

The sp^{2}c-COFs have been in the limelight in the development of next-generation advanced COFs over the past few years. In this review, we have comprehensively overviewed the recent advances in the development of sp^{2}c-COFs. The diverse chemistry toolbox coupled with the reticular synthesis has furnished an increasing number of sp^{2}c-COFs since 2016. The unmatchable structural merits of chemical stability, crystallinity, synthetic availability, continuous π-conjugation, photoluminescence, and atomic-level modularity have established sp^{2}c-COFs as a versatile material platform for a widespread range of applications including heterogeneous catalysis, radionuclides sequestration, lithium-ion batteries, supercapacitors, information encryption, white LEDs, and chemosensors. Despite all these initial accomplishments within such a short period, this field is far from mature with several major challenges that must be tackled to achieve the fullest potential of these materials.

(1) The lack of thorough mechanistic understanding of sp^{2}c-COFs formation hinders the predictive synthesis and rational upgrading of COFs. Whether the crystallization pathway of sp^{2}c-COFs resembles those of boronate ester- and imine-linked COFs or not remains to be explored. We envision that a powerful combination of experiment, characterization, and computation such as scrambling test, kinetic studies, *in-situ* chemical probes, and computational simulations will undoubtedly shed more light on the crystallization process of sp^{2}c-COFs.

(2) The fundamental insight into the photophysical properties of sp^{2}c-COFs is of utter significance for the rational design, synthesis, and exploitation of emissive COFs through establishing direct structure-luminescence relationships. In this regard, a synergistic engagement of advanced spectroscopic characterizations such as femtosecond transient absorption spectroscopy and computational investigations is expected to

Please do not adjust margins

provide a panoramic view of key parameters such as excited states, exciton interactions, and relaxation dynamics, which will decipher the origin of optical behaviors of sp^2c-COFs.

(3) The sluggish solvothermal synthesis with lengthy reaction times (3-5 days) greatly impedes the discovery and practical utility of sp^2c-COFs. Developing broadly applicable approaches that enable the expeditious synthesis of sp^2c-COFs through innovations in energy sources such as mechanical agitation and microwave irradiation, monomers, catalysts, and activation protocols like supercritical CO_2 activation is highly demanded.[130]

(4) The limited scope of sp^2c-COF applications, which are dominated by photocatalysis and uranium sequestration, necessitates the exploration of sp^2c-COFs in other fields wherein imine-linked COFs have been widely exploited such as gas separation,[131] sensing,[132-134] proton conduction,[135] drug delivery,[136] chiral chemistry,[137] and optoelectronics.[54] The advancement of sp^2c-COFs in cutting-edge applications will certainly harness their fullest potential and propel the development of new COFs.

(5) sp^2c-COFs developed thus far dominantly adopt 2D conformation with uniform pores except for a single example of kagome-type sp^2c-COF-5.[49] Hence, developing heteropore sp^2c-COFs with hierarchical porosities and innovative functions merits more efforts in the future.[138] Further, the exploration of 3D COFs remains uncharted yet highly desired.[139]

(6) sp^2c-COFs are mostly aggregated brittle powders with nonprocessability, which is thought of as a roadblock in their practical utility in catalysis, water remediation, and optoelectronic applications.[140] Developing sp^2c-COF thin films[141] or processable COF-polymer composites[142] is largely underexplored and worth more efforts.

(7) To further enhance the structural complexity and chemical stability of sp^2c-COFs, chemical manipulation of sp^2-carbon linkages by either PSM or one-pot cascade reactions offers a viable means to achieve these goals.[143] At the present, the PSM of sp^2c-COFs mostly concentrated on the chemical conversion of pedant cyano groups into amidoxime moieties except for two latest reports on the direct reduction[129] and light-induced [2+2] cycloaddition of sp^2 C=C linkages.[144] Beyond PSM, a unique one-pot cascade reaction that combined Knoevenagel condensation, cyanide shift, ring-closure, and oxidation led to unprecedented benzofuran-linked COFs.[145] We envision that the chemical manipulation of sp^2 C=C linkages will pave a new route to radically new COFs with compelling materials properties.

The designed synthesis of novel sp^2c-COFs will continue to be the frontier of COF research due to their unrivalled combination of crystallinity, porosity, stability, modularity, and functionality. We envision the portfolio of sp^2c-COFs will be further diversified to compete with the dominant imine-linked COFs by means of developing a new library of monomers and the PSM of established sp^2c-COFs. This discovery process of sp^2c-COFs will be greatly accelerated by innovations in energy source, monomer design, catalyst, nucleation control, and workup activation as well as computational high-throughput screening.[146] Moreover, developing sp^2c-COF-based composites by the synergistic integration of COFs and functional materials such as metal nanoparticles, enzymes, MOFs, and polymers is still in its nascent stage yet merits more scientific efforts. Last but not the least, an in-depth mechanistic understanding of the formation and emergent performance in specialty applications is of paramount importance for the mechanism-based synthesis and rational improvement of sp^2c-COFs. Though being in a nascent stage, continuous and interdisciplinary scientific endeavors along these promising directions will lay a solid groundwork for the bright future of sp^2c-COFs.

Conflicts of interest

There are no conflicts to declare.

Acknowledgements

The author acknowledges the support from the U.S. Department of Defense, the Office of Naval Research under the award no: N00014-20-1-2523. The author is grateful for Dr. Yi Liu's guidance during his postdoc training in the Molecular Foundry at Lawrence Berkeley National Laboratory. The author also thanks Dr. Sizhuo Yang and Dr. Chongqing Yang from the Molecular Foundry for the helpful discussions.

References

1. Chen, X.; Geng, K.; Liu, R.; Tan, K. T.; Gong, Y.; Li, Z.; Tao, S.; Jiang, Q.; Jiang, D., Covalent Organic Frameworks: Chemical Approaches to Designer Structures and Built-In Functions. *Angew. Chem. Int. Ed.* **2020**, *59*, 5050-5091.

2. Cote, A. P.; Benin, A. I.; Ockwig, N. W.; O'Keeffe, M.; Matzger, A. J.; Yaghi, O. M., Porous, crystalline, covalent organic frameworks. *Science* **2005**, *310*, 1166-1170.

3. Diercks, C. S.; Yaghi, O. M., The atom, the molecule, and the covalent organic framework. *Science* **2017**, *355*, eaal1585.

4. Geng, K.; He, T.; Liu, R.; Dalapati, S.; Tan, K. T.; Li, Z.; Tao, S.; Gong, Y.; Jiang, Q.; Jiang, D., Covalent Organic Frameworks: Design, Synthesis, and Functions. *Chem. Rev.* **2020**, *120*, 8814-8933.

5. Song, Y.; Sun, Q.; Aguila, B.; Ma, S., Opportunities of covalent organic frameworks for advanced applications. *Adv. Sci.* **2019**, *6*, 1801410.

6. Lohse, M. S.; Bein, T., Covalent organic frameworks: structures, synthesis, and applications. *Adv. Funct. Mater.* **2018**, *28*, 1705553.

7. Kandambeth, S.; Dey, K.; Banerjee, R., Covalent Organic Frameworks: Chemistry beyond the Structure. *J. Am. Chem. Soc.* **2019**, *141*, 1807-1822.

8. Ma, C.; Li, X.; Zhang, J.; Liu, Y.; Urban, J. J., Pyrazine-Fused Porous Graphitic Framework-Based Mixed Matrix Membranes for Enhanced Gas Separations. *ACS Appl. Mater. Interfaces* **2020**, *12*, 16922-16929.

9. Hu, J.; Gupta, S. K.; Ozdemir, J.; Beyzavi, M. H., Applications of Dynamic Covalent Chemistry Concept toward Tailored Covalent Organic Framework Nanomaterials: A Review. *ACS Appl. Nano Mater.* **2020**, *3*, 6239-6269.

10. Liu, W.; Luo, X.; Bao, Y.; Liu, Y. P.; Ning, G.-H.; Abdelwahab, I.; Li, L.; Nai, C. T.; Hu, Z. G.; Zhao, D.; Liu, B.; Quek, S. Y.; Loh, K. P., A two-dimensional conjugated aromatic polymer via C–C coupling reaction. *Nat. Chem.* **2017**, *9*, 563-570.

11. Zhou, D.; Tan, X.; Wu, H.; Tian, L.; Li, M., Synthesis of C− C Bonded Two-Dimensional Conjugated Covalent Organic

This journal is © The Royal Society of Chemistry 20xx

Please do not adjust margins

Framework Films by Suzuki Polymerization on a Liquid–Liquid Interface. *Angew. Chem.* **2019**, *131*, 1390-1395.
12. Wu, S.; Li, M.; Phan, H.; Wang, D.; Herng, T. S.; Ding, J.; Lu, Z.; Wu, J., Toward Two-Dimensional π-Conjugated Covalent Organic Radical Frameworks. *Angew. Chem. Int. Ed.* **2018**, *57*, 8007-8011.
13. Zhang, B.; Wei, M.; Mao, H.; Pei, X.; Alshmimri, S. A.; Reimer, J. A.; Yaghi, O. M., Crystalline dioxin-linked covalent organic frameworks from irreversible reactions. *J. Am. Chem. Soc.* **2018**, *140*, 12715-12719.
14. Huang, X.; Sun, C.; Feng, X., Crystallinity and stability of covalent organic frameworks. *Sci. China Chem.* **2020**, *63*, 1367-1390.
15. Li, X.; Cai, S.; Sun, B.; Yang, C.; Zhang, J.; Liu, Y., Chemically Robust Covalent Organic Frameworks: Progress and Perspective. *Matter* **2020**, *3*, 1507-1540.
16. Guan, X.; Li, H.; Ma, Y.; Xue, M.; Fang, Q.; Yan, Y.; Valtchev, V.; Qiu, S., Chemically stable polyarylether-based covalent organic frameworks. *Nat. Chem.* **2019**, *11*, 587-594.
17. Li, X.; Wang, H.; Chen, H.; Zheng, Q.; Zhang, Q.; Mao, H.; Liu, Y.; Cai, S.; Sun, B.; Dun, C., Dynamic covalent synthesis of crystalline porous graphitic frameworks. *Chem* **2020**, *6*, 933-944.
18. Huang, N.; Lee, K. H.; Yue, Y.; Xu, X.; Irle, S.; Jiang, Q.; Jiang, D., A Stable and Conductive Metallophthalocyanine Framework for Electrocatalytic Carbon Dioxide Reduction in Water. *Angew. Chem. Int. Ed.* **2020**, *59*, 16587-16593.
19. Zhao, C.; Lyu, H.; Ji, Z.; Zhu, C.; Yaghi, O. M., Ester-Linked Crystalline Covalent Organic Frameworks. *J. Am. Chem. Soc.* **2020**, *142*, 14450-14454.
20. Zhang, K.; Cai, S.-L.; Yan, Y.-L.; He, Z.-H.; Lin, H.-M.; Huang, X.-L.; Zheng, S.-R.; Fan, J.; Zhang, W.-G., Construction of a hydrazone-linked chiral covalent organic framework–silica composite as the stationary phase for high performance liquid chromatography. *J. Chromatogr. A* **2017**, *1519*, 100-109.
21. Kandambeth, S.; Mallick, A.; Lukose, B.; Mane, M. V.; Heine, T.; Banerjee, R., Construction of crystalline 2D covalent organic frameworks with remarkable chemical (acid/base) stability via a combined reversible and irreversible route. *J. Am. Chem. Soc.* **2012**, *134*, 19524-19527.
22. Wei, P.-F.; Qi, M.-Z.; Wang, Z.-P.; Ding, S.-Y.; Yu, W.; Liu, Q.; Wang, L.-K.; Wang, H.-Z.; An, W.-K.; Wang, W., Benzoxazole-linked ultrastable covalent organic frameworks for photocatalysis. *J. Am. Chem. Soc.* **2018**, *140*, 4623-4631.
23. Wang, K.; Jia, Z.; Bai, Y.; Wang, X.; Hodgkiss, S. E.; Chen, L.; Chong, S. Y.; Wang, X.; Yang, H.; Xu, Y.; Feng, F.; Ward, J. W.; Cooper, A. I., Synthesis of Stable Thiazole-Linked Covalent Organic Frameworks via a Multicomponent Reaction. *J. Am. Chem. Soc.* **2020**, *142*, 11131-11138.
24. Wang, P.-L.; Ding, S.-Y.; Zhang, Z.-C.; Wang, Z.-P.; Wang, W., Constructing Robust Covalent Organic Frameworks via Multicomponent Reactions. *J. Am. Chem. Soc.* **2019**, *141*, 18004-18008.
25. Li, X.; Zhang, C.; Cai, S.; Lei, X.; Altoe, V.; Hong, F.; Urban, J. J.; Ciston, J.; Chan, E. M.; Liu, Y., Facile transformation of imine covalent organic frameworks into ultrastable crystalline porous aromatic frameworks. *Nat. Commun.* **2018**, *9*, 2998.
26. Seo, J.-M.; Noh, H.-J.; Jeong, H. Y.; Baek, J.-B., Converting Unstable Imine-Linked Network into Stable Aromatic Benzoxazole-Linked One via Post-oxidative Cyclization. *J. Am. Chem. Soc.* **2019**, *141*, 11786-11790.
27. Haase, F.; Troschke, E.; Savasci, G.; Banerjee, T.; Duppel, V.; Dörfler, S.; Grundei, M. M. J.; Burow, A. M.; Ochsenfeld, C.; Kaskel, S.; Lotsch, B. V., Topochemical conversion of an imine- into a thiazole-linked covalent organic framework enabling real structure analysis. *Nat. Commun.* **2018**, *9*, 2600.
28. Wang, Y.; Liu, H.; Pan, Q.; Wu, C.; Hao, W.; Xu, J.; Chen, R.; Liu, J.; Li, Z.; Zhao, Y., Construction of Fully Conjugated Covalent Organic Frameworks via Facile Linkage Conversion for Efficient Photoenzymatic Catalysis. *J. Am. Chem. Soc.* **2020**, *142*, 5958-5963.
29. Acharjya, A.; Pachfule, P.; Roeser, J.; Schmitt, F. J.; Thomas, A., Vinylene-Linked Covalent Organic Frameworks by Base-Catalyzed Aldol Condensation. *Angew. Chem. Int. Ed.* **2019**, *58*, 14865-14870.
30. Zhuang, X.; Zhao, W.; Zhang, F.; Cao, Y.; Liu, F.; Bi, S.; Feng, X., A two-dimensional conjugated polymer framework with fully sp 2-bonded carbon skeleton. *Polym. Chem.* **2016**, *7*, 4176-4181.
31. Jin, E.; Asada, M.; Xu, Q.; Dalapati, S.; Addicoat, M. A.; Brady, M. A.; Xu, H.; Nakamura, T.; Heine, T.; Chen, Q.; Jiang, D., Two-dimensional sp² carbon–conjugated covalent organic frameworks. *Science* **2017**, *357*, 673-676.
32. Zhang, Q.; Dai, M.; Shao, H.; Tian, Z.; Lin, Y.; Chen, L.; Zeng, X. C., Insights into High Conductivity of the Two-Dimensional Iodine-Oxidized sp2-c-COF. *ACS Appl. Mater. Interfaces* **2018**, *10*, 43595-43602.
33. Cui, B.; Zheng, X.; Wang, J.; Liu, D.; Xie, S.; Huang, B., Realization of Lieb lattice in covalent-organic frameworks with tunable topology and magnetism. *Nat. Commun.* **2020**, *11*, 66.
34. Liang, R.-R.; Jiang, S.-Y.; A, R.-H.; Zhao, X., Two-dimensional covalent organic frameworks with hierarchical porosity. *Chem. Soc. Rev.* **2020**, *49*, 3920-3951.
35. Han, X.; Yuan, C.; Hou, B.; Liu, L.; Li, H.; Liu, Y.; Cui, Y., Chiral covalent organic frameworks: design, synthesis and property. *Chem. Soc. Rev.* **2020**, *49*, 6248-6272.
36. Vardhan, H.; Nafady, A.; Al-Enizi, A. M.; Ma, S., Pore surface engineering of covalent organic frameworks: structural diversity and applications. *Nanoscale* **2019**, *11*, 21679-21708.
37. Li, Y.; Chen, W.; Xing, G.; Jiang, D.; Chen, L., New synthetic strategies toward covalent organic frameworks. *Chem. Soc. Rev.* **2020**, *49*, 2852-2868.
38. Yuan, S.; Li, X.; Zhu, J.; Zhang, G.; Van Puyvelde, P.; Van der Bruggen, B., Covalent organic frameworks for membrane separation. *Chem. Soc. Rev.* **2019**, *48*, 2665-2681.
39. Wang, Z.; Zhang, S.; Chen, Y.; Zhang, Z.; Ma, S., Covalent organic frameworks for separation applications. *Chem. Soc. Rev.* **2020**, *49*, 708-735.
40. Zhi, Y.; Wang, Z.; Zhang, H. L.; Zhang, Q., Recent Progress

in Metal-Free Covalent Organic Frameworks as Heterogeneous Catalysts. *Small*, 2001070.
41. Wang, D.-G.; Qiu, T.; Guo, W.; Liang, Z.; Tabassum, H.; Xia, D.; Zou, R., Covalent Organic Framework-Based Materials for Energy Applications. *Energy Environ. Sci.* **2020**.
42. Huang, N.; Wang, P.; Jiang, D., Covalent organic frameworks: a materials platform for structural and functional designs. *Nat. Rev. Mater.* **2016**, *1*, 16068.
43. Bi, S.; Lan, Z.-A.; Paasch, S.; Zhang, W.; He, Y.; Zhang, C.; Liu, F.; Wu, D.; Zhuang, X.; Brunner, E.; Wang, X.; Zhang, F., Substantial Cyano-Substituted Fully sp2-Carbon-Linked Framework: Metal-Free Approach and Visible-Light-Driven Hydrogen Evolution. *Adv. Funct. Mater.* **2017**, *27*, 1703146.
44. Park, J. H.; Ko, K. C.; Park, N.; Shin, H.-W.; Kim, E.; Kang, N.; Hong Ko, J.; Lee, S. M.; Kim, H. J.; Ahn, T. K.; Lee, J. Y.; Son, S. U., Microporous organic nanorods with electronic push–pull skeletons for visible light-induced hydrogen evolution from water. *J. Mater. Chem. A* **2014**, *2*, 7656-7661.
45. Wei, Y.; Chen, W.; Zhao, X.; Ding, S.; Han, S.; Chen, L., Solid-state emissive cyanostilbene based conjugated microporous polymers via cost-effective Knoevenagel polycondensation. *Polym. Chem.* **2016**, *7*, 3983-3988.
46. Yassin, A.; Trunk, M.; Czerny, F.; Fayon, P.; Trewin, A.; Schmidt, J.; Thomas, A., Structure–Thermodynamic-Property Relationships in Cyanovinyl-Based Microporous Polymer Networks for the Future Design of Advanced Carbon Capture Materials. *Adv. Funct. Mater.* **2017**, *27*, 1700233.
47. Lyu, H.; Diercks, C. S.; Zhu, C.; Yaghi, O. M., Porous crystalline olefin-linked covalent organic frameworks. *J. Am. Chem. Soc.* **2019**, *141*, 6848-6852.
48. Yang, Y.; Niu, H.; Xu, L.; Zhang, H.; Cai, Y., Triazine functionalized fully conjugated covalent organic framework for efficient photocatalysis. *Appl. Catal., B* **2020**, *269*, 118799.
49. Jin, E.; Geng, K.; Lee, K. H.; Jiang, W.; Li, J.; Jiang, Q.; Irle, S.; Jiang, D., Topology-Templated Synthesis of Crystalline Porous Covalent Organic Frameworks. *Angew. Chem.* **2020**, *132*, 12260 – 12267.
50. Acharjya, A.; Longworth-Dunbar, L.; Roeser, J.; Pachfule, P.; Thomas, A., Synthesis of Vinylene-Linked Covalent Organic Frameworks from Acetonitrile: Combining Cyclotrimerization and Aldol Condensation in One Pot. *J. Am. Chem. Soc.* **2020**, *142*, 14033-14038.
51. Haase, F.; Lotsch, B. V., Solving the COF trilemma: towards crystalline, stable and functional covalent organic frameworks. *Chem. Soc. Rev.* **2020**, *49*, 8469-8500.
52. Liu, M.; Guo, L.; Jin, S.; Tan, B., Covalent triazine frameworks: synthesis and applications. *J. Mater. Chem. A* **2019**, *7*, 5153-5172.
53. Meng, Z.; Aykanat, A.; Mirica, K. A., Proton Conduction in 2D Aza-Fused Covalent Organic Frameworks. *Chem. Mater.* **2019**, *31*, 819-825.
54. Sun, B.; Li, X.; Feng, T.; Cai, S.; Chen, T.; Zhu, C.; Zhang, J.; Wang, D.; Liu, Y., Resistive Switching Memory Performance of Two-Dimensional Polyimide Covalent Organic Framework Films. *ACS Appl. Mater. Interfaces* **2020**, *12*, 51837-51845.
55. Ranjeesh, K. C.; Illathvalappil, R.; Veer, S. D.; Peter, J.; Wakchaure, V. C.; Goudappagouda; Raj, K. V.; Kurungot, S.; Babu, S. S., Imidazole-Linked Crystalline Two-Dimensional Polymer with Ultrahigh Proton-Conductivity. *J. Am. Chem. Soc.* **2019**, *141*, 14950-14954.
56. Jiang, D., Covalent Organic Frameworks: An Amazing Chemistry Platform for Designing Polymers. *Chem* **2020**, *6*, 2461-2483.
57. Liu, X.; Huang, D.; Lai, C.; Zeng, G.; Qin, L.; Wang, H.; Yi, H.; Li, B.; Liu, S.; Zhang, M.; Deng, R.; Fu, Y.; Li, L.; Xue, W.; Chen, S., Recent advances in covalent organic frameworks (COFs) as a smart sensing material. *Chem. Soc. Rev.* **2019**, *48*, 5266-5302.
58. Gao, Q.; Li, X.; Ning, G.-H.; Leng, K.; Tian, B.; Liu, C.; Tang, W.; Xu, H.-S.; Loh, K. P., Highly photoluminescent two-dimensional imine-based covalent organic frameworks for chemical sensing. *Chem.Comm.* **2018**, *54*, 2349-2352.
59. Dalapati, S.; Jin, E.; Addicoat, M.; Heine, T.; Jiang, D., Highly Emissive Covalent Organic Frameworks. *J. Am. Chem. Soc.* **2016**, *138*, 5797-5800.
60. Crowe, J. W.; Baldwin, L. A.; McGrier, P. L., Luminescent Covalent Organic Frameworks Containing a Homogeneous and Heterogeneous Distribution of Dehydrobenzoannulene Vertex Units. *J. Am. Chem. Soc.* **2016**, *138*, 10120-10123.
61. Dalapati, S.; Jin, S.; Gao, J.; Xu, Y.; Nagai, A.; Jiang, D., An Azine-Linked Covalent Organic Framework. *J. Am. Chem. Soc.* **2013**, *135*, 17310-17313.
62. Jadhav, T.; Fang, Y.; Patterson, W.; Liu, C. H.; Hamzehpoor, E.; Perepichka, D. F., 2D poly (arylene vinylene) covalent organic frameworks via aldol condensation of trimethyltriazine. *Angew. Chem. Int. Ed.* **2019**, *58*, 13753-13757.
63. Jin, E.; Li, J.; Geng, K.; Jiang, Q.; Xu, H.; Xu, Q.; Jiang, D., Designed synthesis of stable light-emitting two-dimensional sp2 carbon-conjugated covalent organic frameworks. *Nat. Commun.* **2018**, *9*, 4143.
64. Xu, S.; Li, Y.; Biswal, B. P.; Addicoat, M. A.; Paasch, S.; Imbrasas, P.; Park, S.; Shi, H.; Brunner, E.; Richter, M.; Lenk, S.; Reineke, S.; Feng, X., Luminescent sp2-Carbon-Linked 2D Conjugated Polymers with High Photostability. *Chem. Mater.* **2020**, *32*, 7985-7991.
65. Segura, J. L.; Mancheño, M. J.; Zamora, F., Covalent organic frameworks based on Schiff-base chemistry: synthesis, properties and potential applications. *Chem. Soc. Rev.* **2016**, *45*, 5635-5671.
66. Castano, I.; Evans, A. M.; Li, H.; Vitaku, E.; Strauss, M. J.; Brédas, J.-L.; Gianneschi, N. C.; Dichtel, W. R., Chemical Control over Nucleation and Anisotropic Growth of Two-Dimensional Covalent Organic Frameworks. *ACS Cent. Sci.* **2019**, *5*, 1892-1899.
67. Smith, B. J.; Overholts, A. C.; Hwang, N.; Dichtel, W. R., Insight into the crystallization of amorphous imine-linked polymer networks to 2D covalent organic frameworks. *Chem.Comm.* **2016**, *52*, 3690-3693.
68. Feriante, C.; Evans, A. M.; Jhulki, S.; Castano, I.; Strauss, M. J.; Barlow, S.; Dichtel, W. R.; Marder, S. R., New Mechanistic Insights into the Formation of Imine-Linked Two-Dimensional

This journal is © The Royal Society of Chemistry 20xx

Please do not adjust margins

Covalent Organic Frameworks. *J. Am. Chem. Soc.* **2020**, *142*, 18637-18644.
69. Kulchat, S.; Meguellati, K.; Lehn, J.-M., Organocatalyzed and Uncatalyzed C=C/C=C and C=C/C=N Exchange Processes between Knoevenagel and Imine Compounds in Dynamic Covalent Chemistry. *Helvetica Chimica Acta* **2014**, *97*, 1219-1236.
70. Gu, R.; Flidrova, K.; Lehn, J.-M., Dynamic Covalent Metathesis in the C=C/C=N Exchange between Knoevenagel Compounds and Imines. *J. Am. Chem. Soc.* **2018**, *140*, 5560-5568.
71. Becker, D.; Biswal, B. P.; Kaleńczuk, P.; Chandrasekhar, N.; Giebeler, L.; Addicoat, M.; Paasch, S.; Brunner, E.; Leo, K.; Dianat, A.; Cuniberti, G.; Berger, R.; Feng, X., Fully sp2-Carbon-Linked Crystalline Two-Dimensional Conjugated Polymers: Insight into 2D Poly(phenylenecyanovinylene) Formation and its Optoelectronic Properties. *Chem. Eur. J.* **2019**, *25*, 6562-6568.
72. Pastoetter, D. L.; Xu, S.; Borrelli, M.; Addicoat, M.; Biswal, B. P.; Paasch, S.; Dianat, A.; Thomas, H.; Berger, R.; Reineke, S.; Brunner, E.; Cuniberti, G.; Richter, M.; Feng, X., Synthesis of Vinylene-Linked Two-Dimensional Conjugated Polymers via the Horner–Wadsworth–Emmons Reaction. *Angew. Chem. Int. Ed.* **2020**, *59*, 23620-23625.
73. Ong, W. J.; Swager, T. M., Dynamic self-correcting nucleophilic aromatic substitution. *Nat. Chem.* **2018**, *10*, 1023-1030.
74. Smith, B. J.; Dichtel, W. R., Mechanistic studies of two-dimensional covalent organic frameworks rapidly polymerized from initially homogenous conditions. *J. Am. Chem. Soc.* **2014**, *136*, 8783-8789.
75. Li, Rebecca L.; Flanders, N. C.; Evans, A. M.; Ji, W.; Castano, I.; Chen, L. X.; Gianneschi, N. C.; Dichtel, W. R., Controlled growth of imine-linked two-dimensional covalent organic framework nanoparticles. *Chem. Sci.* **2019**, *10*, 3796-3801.
76. Li, H.; Chavez, A. D.; Li, H.; Li, H.; Dichtel, W. R.; Bredas, J.-L., Nucleation and Growth of Covalent Organic Frameworks from Solution: The Example of COF-5. *J. Am. Chem. Soc.* **2017**, *139*, 16310-16318.
77. McAtee, R. C.; McClain, E. J.; Stephenson, C. R., Illuminating photoredox catalysis. *Trends Chem.* **2019**, *1*, 111-125.
78. Opoku, F.; Govender, K. K.; van Sittert, C. G. C. E.; Govender, P. P., Recent Progress in the Development of Semiconductor-Based Photocatalyst Materials for Applications in Photocatalytic Water Splitting and Degradation of Pollutants. *Advanced Sustainable Systems* **2017**, *1*, 1700006.
79. Xiao, J.-D.; Jiang, H.-L., Metal–Organic Frameworks for Photocatalysis and Photothermal Catalysis. *Acc. Chem. Res.* **2019**, *52*, 356-366.
80. Zhang, T.; Xing, G.; Chen, W.; Chen, L., Porous organic polymers: a promising platform for efficient photocatalysis. *Mater. Chem. Front.* **2020**, *4*, 332-353.
81. Yang, Q.; Luo, M.; Liu, K.; Cao, H.; Yan, H., Covalent organic frameworks for photocatalytic applications. *Appl. Catal., B* **2020**, *276*, 119174.
82. Stegbauer, L.; Schwinghammer, K.; Lotsch, B. V., A hydrazone-based covalent organic framework for photocatalytic hydrogen production. *Chem. Sci.* **2014**, *5*, 2789-2793.
83. Wang, G.-B.; Li, S.; Yan, C.-X.; Zhu, F.-C.; Lin, Q.-Q.; Xie, K.-H.; Geng, Y.; Dong, Y.-B., Covalent organic frameworks: emerging high-performance platforms for efficient photocatalytic applications. *J. Mater. Chem. A* **2020**, *8*, 6957-6983.
84. Jin, E.; Lan, Z.; Jiang, Q.; Geng, K.; Li, G.; Wang, X.; Jiang, D., 2D sp2 carbon-conjugated covalent organic frameworks for photocatalytic hydrogen production from water. *Chem* **2019**, *5*, 1632-1647.
85. Bi, S.; Yang, C.; Zhang, W.; Xu, J.; Liu, L.; Wu, D.; Wang, X.; Han, Y.; Liang, Q.; Zhang, F., Two-dimensional semiconducting covalent organic frameworks via condensation at arylmethyl carbon atoms. *Nat. Commun.* **2019**, *10*, 1-10.
86. Vyas, V. S.; Haase, F.; Stegbauer, L.; Savasci, G.; Podjaski, F.; Ochsenfeld, C.; Lotsch, B. V., A tunable azine covalent organic framework platform for visible light-induced hydrogen generation. *Nat. Commun.* **2015**, *6*, 8508.
87. Wang, X.; Chen, L.; Chong, S. Y.; Little, M. A.; Wu, Y.; Zhu, W.-H.; Clowes, R.; Yan, Y.; Zwijnenburg, M. A.; Sprick, R. S.; Cooper, A. I., Sulfone-containing covalent organic frameworks for photocatalytic hydrogen evolution from water. *Nat. Chem.* **2018**, *10*, 1180-1189.
88. Wei, S.; Zhang, F.; Zhang, W.; Qiang, P.; Yu, K.; Fu, X.; Wu, D.; Bi, S.; Zhang, F., Semiconducting 2D Triazine-cored covalent organic frameworks with unsubstituted olefin linkages. *J. Am. Chem. Soc.* **2019**, *141*, 14272-14279.
89. Xu, J.; Yang, C.; Bi, S.; Wang, W.; He, Y.; Wu, D.; Liang, Q.; Wang, X.; Zhang, F., Vinylene-Linked Covalent Organic Frameworks (COFs) with Symmetry-Tuned Polarity and Photocatalytic Activity. *Angew. Chem. Int. Ed.* **2020**, *59*, 23845-23853.
90. Xu, S.; Sun, H.; Addicoat, M.; Biswal, B. P.; He, F.; Park, S.; Paasch, S.; Zhang, T.; Sheng, W.; Brunner, E.; Hou, Y.; Richter, M.; Feng, X., Thiophene-Bridged Donor–Acceptor sp2-Carbon-Linked 2D Conjugated Polymers as Photocathodes for Water Reduction. *Adv. Mater.* **2021**, *33*, 2006274.
91. Mo, C.; Yang, M.; Sun, F.; Jian, J.; Zhong, L.; Fang, Z.; Feng, J.; Yu, D., Alkene-Linked Covalent Organic Frameworks Boosting Photocatalytic Hydrogen Evolution by Efficient Charge Separation and Transfer in the Presence of Sacrificial Electron Donors. *Adv. Sci.* **2020**, 1902988.
92. Kong, T.; Jiang, Y.; Xiong, Y., Photocatalytic CO2 conversion: What can we learn from conventional COx hydrogenation? *Chem. Soc. Rev.* **2020**, *49*, 6579-6591.
93. Fu, Z.; Wang, X.; Gardner, A. M.; Wang, X.; Chong, S. Y.; Neri, G.; Cowan, A. J.; Liu, L.; Li, X.; Vogel, A.; Clowes, R.; Bilton, M.; Chen, L.; Sprick, R. S.; Cooper, A. I., A stable covalent organic framework for photocatalytic carbon dioxide reduction. *Chem. Sci.* **2020**, *11*, 543-550.

94. Xiang, Y.; Dong, W.; Wang, P.; Wang, S.; Ding, X.; Ichihara, F.; Wang, Z.; Wada, Y.; Jin, S.; Weng, Y.; Chen, H.; Ye, J., Constructing electron delocalization channels in covalent organic frameworks powering CO2 photoreduction in water. *Appl. Catal., B* **2020**, *274*, 119096.
95. Wang, H.; Wang, H.; Wang, Z.; Tang, L.; Zeng, G.; Xu, P.; Chen, M.; Xiong, T.; Zhou, C.; Li, X.; Huang, D.; Zhu, Y.; Wang, Z.; Tang, J., Covalent organic framework photocatalysts: structures and applications. *Chem. Soc. Rev.* **2020**, *49*, 4135-4165.
96. Chen, R.; Shi, J.-L.; Ma, Y.; Lin, G.; Lang, X.; Wang, C., Designed Synthesis of a 2D Porphyrin-Based sp2 Carbon-Conjugated Covalent Organic Framework for Heterogeneous Photocatalysis. *Angew. Chem. Int. Ed.* **2019**, *58*, 6430-6434.
97. Shi, J.-L.; Chen, R.; Hao, H.; Wang, C.; Lang, X., 2D sp2 Carbon-Conjugated Porphyrin Covalent Organic Framework for Cooperative Photocatalysis with TEMPO. *Angew. Chem. Int. Ed.* **2020**, *59*, 9088-9093.
98. Li, S.; Li, L.; Li, Y.; Dai, L.; Liu, C.; Liu, Y.; Li, J.; Lv, J.; Li, P.; Wang, B., Fully Conjugated Donor–Acceptor Covalent Organic Frameworks for Photocatalytic Oxidative Amine Coupling and Thioamide Cyclization. *ACS Catal.* **2020**, *10*, 8717-8726.
99. Zhao, Y.; Liu, H.; Wu, C.; Zhang, Z.; Pan, Q.; Hu, F.; Wang, R.; Li, P.; Huang, X.; Li, Z., Fully Conjugated Two-Dimensional sp2-Carbon Covalent Organic Frameworks as Artificial Photosystem I with High Efficiency. *Angew. Chem. Int. Ed.* **2019**, *58*, 5376-5381.
100. Bi, S.; Thiruvengadam, P.; Wei, S.; Zhang, W.; Zhang, F.; Gao, L.; Xu, J.; Wu, D.; Chen, J.-S.; Zhang, F., Vinylene-Bridged Two-Dimensional Covalent Organic Frameworks via Knoevenagel Condensation of Tricyanomesitylene. *J. Am. Chem. Soc.* **2020**, *142*, 11893-11900.
101. Banerjee, T.; Podjaski, F.; Kröger, J.; Biswal, B. P.; Lotsch, B. V., Polymer photocatalysts for solar-to-chemical energy conversion. *Nat. Rev. Mater.* **2020**.
102. Guo, J.; Jiang, D., Covalent Organic Frameworks for Heterogeneous Catalysis: Principle, Current Status, and Challenges. *ACS Cent. Sci.* **2020**, *6*, 869-879.
103. Zhai, L.; Yang, S.; Yang, X.; Ye, W.; Wang, J.; Chen, W.; Guo, Y.; Mi, L.; Wu, Z.; Soutis, C.; Xu, Q.; Jiang, Z., Conjugated Covalent Organic Frameworks as Platinum Nanoparticle Supports for Catalyzing the Oxygen Reduction Reaction. *Chem. Mater.* **2020**, *32*, 9747-9752.
104. Lin, C.-Y.; Zhang, D.; Zhao, Z.; Xia, Z., Covalent Organic Framework Electrocatalysts for Clean Energy Conversion. *Adv. Mater.* **2018**, *30*, 1703646.
105. Samanta, P.; Desai, A. V.; Let, S.; Ghosh, S. K., Advanced Porous Materials for Sensing, Capture and Detoxification of Organic Pollutants toward Water Remediation. *ACS Sustain. Chem. Eng.* **2019**, *7*, 7456-7478.
106. Fernandes, S. P.; Romero, V.; Espiña, B.; Salonen, L. M., Tailoring Covalent Organic Frameworks To Capture Water Contaminants. *Chem. Eur. J.* **2019**, *25*, 6461-6473.
107. Sun, Q.; Aguila, B.; Ma, S., Opportunities of porous organic polymers for radionuclide sequestration. *Trends Chem.* **2019**, *1*, 292-303.
108. Cui, W.-R.; Zhang, C.-R.; Jiang, W.; Li, F.-F.; Liang, R.-P.; Liu, J.; Qiu, J.-D., Regenerable and stable sp 2 carbon-conjugated covalent organic frameworks for selective detection and extraction of uranium. *Nat. Commun.* **2020**, *11*, 1-10.
109. Sun, Q.; Aguila, B.; Earl, L. D.; Abney, C. W.; Wojtas, L.; Thallapally, P. K.; Ma, S., Covalent Organic Frameworks as a Decorating Platform for Utilization and Affinity Enhancement of Chelating Sites for Radionuclide Sequestration. *Adv. Mater.* **2018**, *30*, 1705479.
110. Li, X.; Qi, Y.; Yue, G.; Wu, Q.; Li, Y.; Zhang, M.; Guo, X.; Li, X.; Ma, L.; Li, S., Solvent- and catalyst-free synthesis of an azine-linked covalent organic framework and the induced tautomerization in the adsorption of U(vi) and Hg(ii). *Green Chem.* **2019**, *21*, 649-657.
111. Zhang, C.-R.; Cui, W.-R.; Jiang, W.; Li, F.-F.; Wu, Y.-D.; Liang, R.-P.; Qiu, J.-D., Simultaneous sensitive detection and rapid adsorption of UO22+ based on a post-modified sp2 carbon-conjugated covalent organic framework. *Environmental Science: Nano* **2020**, *7*, 842-850.
112. Li, F.-F.; Cui, W.-R.; Jiang, W.; Zhang, C.-R.; Liang, R.-P.; Qiu, J.-D., Stable sp2 carbon-conjugated covalent organic framework for detection and efficient adsorption of uranium from radioactive wastewater. *J. Hazard. Mater.* **2020**, *392*, 122333.
113. Cui, W.-R.; Li, F.-F.; Xu, R.-H.; Zhang, C.-R.; Chen, X.-R.; Yan, R.-H.; Liang, R.-P.; Qiu, J.-D., Regenerable Covalent Organic Frameworks for Photo-enhanced Uranium Adsorption from Seawater. *Angew. Chem. Int. Ed.* **2020**, *59*, 17684-17690.
114. Cui, W.-R.; Zhang, C.-R.; Xu, R.-H.; Chen, X.-R.; Yan, R.-H.; Jiang, W.; Liang, R.-P.; Qiu, J.-D., High-Efficiency Photoenhanced Extraction of Uranium from Natural Seawater by Olefin-Linked Covalent Organic Frameworks. *ACS ES&T Water* **2020**.
115. Zhang, C.-R.; Cui, W.-R.; Xu, R.-H.; Chen, X.-R.; Jiang, W.; Wu, Y.-D.; Yan, R.-H.; Liang, R.-P.; Qiu, J.-D., Alkynyl-Based sp² Carbon-Conjugated Covalent Organic Frameworks with Enhanced Uranium Extraction from Seawater by Photoinduced Multiple Effects. *CCS Chemistry* **2020**.
116. Li, M.; Lu, J.; Chen, Z.; Amine, K., 30 Years of Lithium-Ion Batteries. *Adv. Mater.* **2018**, *30*, 1800561.
117. Lu, Y.; Chen, J., Prospects of organic electrode materials for practical lithium batteries. *Nature Reviews Chemistry* **2020**, *4*, 127-142.
118. Sun, T.; Xie, J.; Guo, W.; Li, D.-S.; Zhang, Q., Covalent–Organic Frameworks: Advanced Organic Electrode Materials for Rechargeable Batteries. *Adv. Energy Mater.* **2020**, *10*, 1904199.
119. Xu, S.; Wang, G.; Biswal, B. P.; Addicoat, M.; Paasch, S.; Sheng, W.; Zhuang, X.; Brunner, E.; Heine, T.; Berger, R.; Feng, X., A Nitrogen-Rich 2D sp2-Carbon-Linked Conjugated Polymer Framework as a High-Performance Cathode for Lithium-Ion Batteries. *Angew. Chem. Int. Ed.* **2019**, *58*, 849-853.

This journal is © The Royal Society of Chemistry 20xx

Please do not adjust margins

120. Peng, C.; Ning, G.-H.; Su, J.; Zhong, G.; Tang, W.; Tian, B.; Su, C.; Yu, D.; Zu, L.; Yang, J.; Ng, M.-F.; Hu, Y.-S.; Yang, Y.; Armand, M.; Loh, K. P., Reversible multi-electron redox chemistry of π-conjugated N-containing heteroaromatic molecule-based organic cathodes. *Nature Energy* **2017**, *2*, 17074.
121. Wang, J.; Tee, K.; Lee, Y.; Riduan, S. N.; Zhang, Y., Hexaazatriphenylene derivatives/GO composites as organic cathodes for lithium ion batteries. *J. Mater. Chem. A* **2018**, *6*, 2752-2757.
122. Wang, J.; Lee, Y.; Tee, K.; Riduan, S. N.; Zhang, Y., A nanoporous sulfur-bridged hexaazatrinaphthylene framework as an organic cathode for lithium ion batteries with well-balanced electrochemical performance. *Chem.Comm.* **2018**, *54*, 7681-7684.
123. González, A.; Goikolea, E.; Barrena, J. A.; Mysyk, R., Review on supercapacitors: Technologies and materials. *Renewable and Sustainable Energy Reviews* **2016**, *58*, 1189-1206.
124. Gao, X.; Dong, Y.; Li, S.; Zhou, J.; Wang, L.; Wang, B., MOFs and COFs for Batteries and Supercapacitors. *Electrochemical Energy Reviews* **2020**, *3*, 81-126.
125. Xu, J.; He, Y.; Bi, S.; Wang, M.; Yang, P.; Wu, D.; Wang, J.; Zhang, F., An Olefin-Linked Covalent Organic Framework as a Flexible Thin-Film Electrode for a High-Performance Micro-Supercapacitor. *Angew. Chem. Int. Ed.* **2019**, *131*, 12193-12197.
126. Zhang, F.; Wei, S.; Wei, W.; Zou, J.; Gu, G.; Wu, D.; Bi, S.; Zhang, F., Trimethyltriazine-derived olefin-linked covalent organic framework with ultralong nanofibers. *Science Bulletin* **2020**, *65*, 1659-1666.
127. Yang, M.; Mo, C.; Fang, L.; Li, J.; Yuan, Z.; Chen, Z.; Jiang, Q.; Chen, X.; Yu, D., Multibranched Octupolar Module Embedded Covalent Organic Frameworks Enable Efficient Two-Photon Fluorescence. *Adv. Funct. Mater.* **2020**, *30*, 2000516.
128. Yang, S.; Streater, D.; Fiankor, C.; Zhang, J.; Huang, J., Conjugation- and Aggregation-Directed Design of Covalent Organic Frameworks as White-Light-Emitting Diodes. *J. Am. Chem. Soc.* **2021**, *143*, 1061-1068.
129. Yuan, C.; Fu, S.; Yang, K.; Hou, B.; Liu, Y.; Jiang, J.; Cui, Y., Crystalline C—C and C═C Bond-Linked Chiral Covalent Organic Frameworks. *J. Am. Chem. Soc.* **2021**, *143*, 369-381.
130. Li, X.; Yang, C.; Sun, B.; Cai, S.; Chen, Z.; Lv, Y.; Zhang, J.; Liu, Y., Expeditious synthesis of covalent organic frameworks: a review. *J. Mater. Chem. A* **2020**, *8*, 16045-16060.
131. Fan, H.; Mundstock, A.; Feldhoff, A.; Knebel, A.; Gu, J.; Meng, H.; Caro, J., Covalent Organic Framework–Covalent Organic Framework Bilayer Membranes for Highly Selective Gas Separation. *J. Am. Chem. Soc.* **2018**, *140*, 10094-10098.
132. Ascherl, L.; Evans, E. W.; Hennemann, M.; Di Nuzzo, D.; Hufnagel, A. G.; Beetz, M.; Friend, R. H.; Clark, T.; Bein, T.; Auras, F., Solvatochromic covalent organic frameworks. *Nat. Commun.* **2018**, *9*, 3802.
133. He, Z.-H.; Gong, S.-D.; Cai, S.-L.; Yan, Y.-L.; Chen, G.; Li, X.-L.; Zheng, S.-R.; Fan, J.; Zhang, W.-G., A Benzimidazole-Containing Covalent Organic Framework-Based QCM Sensor for Exceptional Detection of CEES. *Cryst. Growth Des.* **2019**, *19*, 3543-3550.
134. Chen, G.; Lan, H.-H.; Cai, S.-L.; Sun, B.; Li, X.-L.; He, Z.-H.; Zheng, S.-R.; Fan, J.; Liu, Y.; Zhang, W.-G., Stable Hydrazone-Linked Covalent Organic Frameworks Containing O, N, O'-Chelating Sites for Fe (III) Detection in Water. *ACS Appl. Mater. Interfaces* **2019**, *11*, 12830-12837.
135. Tao, S.; Zhai, L.; Dinga Wonanke, A. D.; Addicoat, M. A.; Jiang, Q.; Jiang, D., Confining H3PO4 network in covalent organic frameworks enables proton super flow. *Nat. Commun.* **2020**, *11*, 1981.
136. Zhang, G.; Li, X.; Liao, Q.; Liu, Y.; Xi, K.; Huang, W.; Jia, X., Water-dispersible PEG-curcumin/amine-functionalized covalent organic framework nanocomposites as smart carriers for in vivo drug delivery. *Nat. Commun.* **2018**, *9*, 2785.
137. Zhuo, S.; Zhang, X.; Luo, H.; Wang, X.; Ji, Y., The Application of Covalent Organic Frameworks for Chiral Chemistry. *Macromol. Rapid Commun.* **2020**, *41*, 2000404.
138. Liang, R.-R.; Zhao, X., Heteropore covalent organic frameworks: a new class of porous organic polymers with well-ordered hierarchical porosities. *Org. Chem. Front.* **2018**, *5*, 3341-3356.
139. Guan, X.; Chen, F.; Fang, Q.; Qiu, S., Design and applications of three dimensional covalent organic frameworks. *Chem. Soc. Rev.* **2020**, *49*, 1357-1384.
140. Rodríguez-San-Miguel, D.; Zamora, F., Processing of covalent organic frameworks: an ingredient for a material to succeed. *Chem. Soc. Rev.* **2019**, *48*, 4375-4386.
141. Wang, H.; Zeng, Z.; Xu, P.; Li, L.; Zeng, G.; Xiao, R.; Tang, Z.; Huang, D.; Tang, L.; Lai, C.; Jiang, D.; Liu, Y.; Yi, H.; Qin, L.; Ye, S.; Ren, X.; Tang, W., Recent progress in covalent organic framework thin films: fabrications, applications and perspectives. *Chem. Soc. Rev.* **2019**, *48*, 488-516.
142. Liu, Y.; Zhou, W.; Teo, W. L.; Wang, K.; Zhang, L.; Zeng, Y.; Zhao, Y., Covalent-Organic-Framework-Based Composite Materials. *Chem* **2020**, *6*, 3172-3202.
143. Ding, H.; Mal, A.; Wang, C., Tailored covalent organic frameworks by post-synthetic modification. *Mater. Chem. Front.* **2020**, *4*, 113-127.
144. Jadhav, T.; Fang, Y.; Liu, C.-H.; Dadvand, A.; Hamzehpoor, E.; Patterson, W.; Jonderian, A.; Stein, R. S.; Perepichka, D. F., Transformation between 2D and 3D Covalent Organic Frameworks via Reversible [2 + 2] Cycloaddition. *J. Am. Chem. Soc.* **2020**, *142*, 8862-8870.
145. Su, Y.; Wan, Y.; Xu, H.; Otake, K.-i.; Tang, X.; Huang, L.; Kitagawa, S.; Gu, C., Crystalline and Stable Benzofuran-Linked Covalent Organic Frameworks from Irreversible Cascade Reactions. *J. Am. Chem. Soc.* **2020**, *142*, 13316-13321.
146. Colón, Y. J.; Snurr, R. Q., High-throughput computational screening of metal–organic frameworks. *Chem. Soc. Rev.* **2014**, *43*, 5735-5749.